

# **Integrative omics and phase IIa clinical trial identify TNF as key node in autoimmune hepatitis**

Yang Xu, Jan Philipp Weltzsch, Christoph Kilian, Babett Steglich, Christina Weiler-Normann, Michael Dudek, Jonas Fackler, Malte H. Wehmeyer, Joseph Tintelnot, Laura A. Liebig, Silja Steinmann, Alena Laschtowitz, Ludwig J. Horst, Ida Schregel, Marcial Sebode, Johannes Hartl, Christian Casar, Jing Lu, Gerhard Schön, Antonia Zapf, Maria Rosa Bono, Mariana V. Roseblatt, Sarah Nuñez, Justine Castañeda, Sören Alexander Weidemann, Nico Kaiser, Maria Schwerk, Manuela Kolster, Guido Rattay, Hanna Ulrich, Varshi Sivayoganathan, Ning Song, Jenny Krause, Marius Böttcher, Adrian Sagebiel, Jonas Wagner, Christian F. Krebs, Victor G. Puelles, Norbert Hübner, Eva Tolosa, Stefan Bonn, Samuel Huber, Percy A. Knolle, Johannes Herkel, Lorenz Adlung, Christoph Schramm, Nicola Gagliani, Ansgar Wilhelm Lohse

## Table of contents

|                               |    |
|-------------------------------|----|
| Supplementary methods.....    | 2  |
| Supplementary references..... | 10 |
| Supplementary tables.....     | 11 |
| Supplementary figures.....    | 25 |

## Supplementary methods

**See Supplementary CTAT Table 1 (page 13) for details on reagents and software packages**

### Multi-omics workflow

**Bulk RNA purification and Sequencing.** Total RNA was extracted from frozen liver tissue using the NucleoSpin Kit (Macherey-Nagel). Complementary DNA (cDNA) was then transcribed from the total RNA using the High-Capacity cDNA Reverse Transcriptase Kit (Thermo Fisher Scientific). The quality was evaluated using Bioanalyzer (Agilent Technologies) and samples with an RNA integrity number < 7 were excluded from further analysis. mRNA libraries were synthesized using Illumina TruSeq Stranded mRNA Library Preparation assay and sequencing were conducted on a HiSeq 4000 system.

**Quantitative real-time PCR.** Total liver RNA was prepared with the NucleoSpin RNA Kit (Macherey-Nagel) according to the manufacturer's instructions. RNA was reverse-transcribed to cDNA with the High-Capacity cDNA Reverse Transcription Kit (Thermo Fisher Scientific). To determine the relative expression level of each gene of interest, qPCR was performed with TaqMan probes and the KAPA PROBE FAST Universal 2X qPCR Master Mix Kit (Roche). RNA expression of target genes was determined with probes from Thermo Fisher Scientific relative to the expression of hypoxanthine-guanine phosphoribosyltransferase (HPRT) (Hs02800695\_m1).

**Alignment, preprocessing and bioinformatic analysis.** The FASTQ files were assessed using FastQC to ensure a proper sequencing quality. Next, TruSeq2-PE adapter and low quality read trimming was performed with Trimmomatic<sup>1</sup> using the options ILLUMINACLIP:TruSeq2-PE.fa:2:30:10:2:falseSLIDINGWINDOW:4:15. STAR was used to align the read against ensemble 87 reference genome and annotation. Bioinformatic and statistical analysis was performed in R. For the sake of reproducibility, the seed was set to 0. If not mentioned otherwise, we run the methods with the default parameters of the respective R package. We only considered genes being expressed in more than 1/3 of our patients. Subsequently, every gene and sample passed WGCNAs method goodSampleGenes. We further removed all genes, which could not be translated to HGNC symbols by biomaRt. DESeq2<sup>2</sup> median of ratio (method estimateSizeFactors) normalization was used to create a normalized count matrix. Variance stabilizing transformation (method vst(blind = TRUE), library DESeq) was applied to calculate principal components (method prcomp). Based on the geneset HALLMARK\_INFLAMMATORY\_RESPONSE provided by the Molecular Signature Database (Human MSigDB v2024.1.Hs, <https://www.gsea-msigdb.org/>) the inflammation

score (Fig. 1c) was obtained. Important gene dynamics in the process of inflammation in patients with AIH were identified by applying rank-based correlation. Therefore, a gene  $\times$  feature correlation matrix with the correlation coefficient (Spearman's rho ( $r_s$ )) between each gene and the feature as elements ( $a_{ij} = r_{s \text{ R}(\text{gene } i)\text{R}(\text{feature } j)}$ ) was constructed. Rank-based correlation was selected because we aimed to capture strictly monotonic behaviour. Furthermore, mHAI values are measured on an ordinal scale. The method `fgsea` from R package `fgsea` was applied to genes ranked with respect to their respective  $r_s$ . Additionally, parent and grandparent terms/categories and the annotated genes were retrieved using the R package `KEGGREST` to group and subset the overrepresented terms. The KEGG pathway maps "Human Diseases" were excluded from the analysis. The R package `decoupleR` was utilized to evaluate the transcription factor activity. Transcription factor activity was determined by the t-statistic of the coefficients of a univariate linear model (method `run_ulm`) based on our input data ( $|r_s| > 0.6$ ) and the CollecTRI gene regulatory network.<sup>3</sup>

**Human liver single cell suspension.** Fresh liver samples were processed independent of disease status. Human liver tissue was rinsed with 0.9% NaCl, and a single-cell suspension was prepared by mechanical fragmentation followed by enzymatic digestion in 10ml RPMI medium (Gibco) containing 10% FBS (PAN Biotech), 0.1mg/ml collagenase D (Roche), 0.1mg/ml DNase I (Roche), 1mM CaCl<sub>2</sub>, and 1mM MgCl<sub>2</sub>. Digestion was performed on a rotary shaker at 180rpm, 37°C for 30 minutes. The suspension was filtered through a 30 $\mu$ m filter, and residual tissue was mechanically disrupted further. The digestion was halted by adding washing buffer containing 1x PBS (Gibco) with 1% FBS and 2mM EDTA (Sigma-Aldrich), followed by centrifugation. The resulting cell pellets were processed for CITE-seq preparation or flow cytometry analysis.

**Human peripheral blood mononuclear cell (PBMC) isolation.** PBMCs were isolated by diluting blood 1:1 with 1x PBS and layering onto equal amounts of Ficoll (Cytiva), followed by centrifugation at 400  $\times$  g, room temperature for 30 minutes. Cells from the interphase layer were collected, washed, and centrifuged. The cell pellets were subsequently processed for CITE-seq preparation or flow cytometry analysis.

### **CITE-seq and snRNA-seq workflow**

**Antibody staining for CITE-seq.** Antibodies for epitope capture in the sequencing workflow are listed in Supplementary (CTAT) table 1. To capture live cells, fixable viability dye eFluor 506 (Thermo Fisher) was used to stain cells on ice for 10 minutes. To minimize nonspecific antibody binding, cells were incubated with Human FC Block (BD Biosciences) together with fluorochrome conjugated anti-human antibodies (BioLegend) on ice for 10 minutes, including

anti-CD45 (clone HI30) for liver single cell suspensions, and anti-CD3 (clone SK7) for PBMCs. Liver samples were further stained with TotalSeq™-C barcode-labelled anti-human antibodies (BioLegend) on ice for 30 mins. PBMCs were stained with TotalSeq™-C Human Universal Cocktail V 1.0 (BioLegend) on ice for 30 minutes. The cells were then washed thoroughly and subjected to FACS sorting.

**Single cell FACS, library preparation and next generation sequencing.** To enrich immune cells from AIH liver single cell suspension, CD45<sup>+</sup> cells were FACS-sorted. CD3<sup>+</sup> T cells were FACS-sorted from paired PBMCs. FACS was conducted using a FACSAria Fusion (BD Bioscience). CITE-seq was performed using the Chromium Controller (10X Genomics). Single-cell libraries were generated using the Chromium Next GEM Single Cell V(D)J Reagent kit v1.1 (10X Genomics), following the manufacturer's instructions. Quality control was conducted using the BioAnalyzer (Agilent). The libraries were sequenced on an Illumina NovaSeq 6000 system.

**Human liver single nuclear suspension.** Frozen liver samples were processed independent of disease status. Nuclei isolation and library preparation were performed at the Max-Delbrück Center for Molecular Medicine as previously described.<sup>4</sup> The following adjustments were made for liver tissue: The homogenization buffer was modified with 0.3% Triton X-100 in nuclease-free water. After filtering, the homogenate was incubated in the buffer for 3 minutes. Single nuclei were purified by FACS using FACSAria (BD Biosciences). Nuclei purity and integrity were confirmed using a microscope and Countess III FL (Life Technologies), which was also used for nuclei counting.

**Single nuclei high-throughput sequencing.** Nuclei were then processed with the Chromium Controller (10X Genomics), targeting 5000–10000 nuclei per reaction. Gene expression libraries were prepared using the Chromium Next GEM Single Cell 3' Reagent Kits v3.1 (10X Genomics). Quality control was performed on final cDNA using the Bioanalyzer (Agilent) and KAPA Library Quantification kit. Libraries were sequenced on an Illumina HiSeq 4000 or NovaSeq, targeting 30000–50000 reads per nucleus.

**Pre-processing of CITE-seq and snRNA-seq data.** The CellRanger software pipeline (v6.1.1, 10X Genomics) was used to demultiplex cellular barcodes and map reads to the human reference genome (GRCh38-2020-A)<sup>5</sup> using the CellRanger count command. For snRNA-seq data, the include-introns option was applied. CITE-seq antibody and barcode information were incorporated via a feature reference CSV file provided to the CellRanger count command. This process generated feature-barcode matrices containing gene

expression and CITE-seq counts for each cell barcode. The feature-barcode matrices for all samples were further analysed in R using Seurat package. During quality control, cells with fewer than 350 detected features in both CITE-seq and snRNA-seq were excluded. Additionally, cells with more than 5% mitochondrial reads in CITE-seq and more than 1% in snRNA-seq were filtered out as low-quality cells. To remove potential doublets of the same cell type, cells with a feature-count ratio below 0.2 were excluded. Doublets of different cell types were identified and filtered using DoubletFinder, with adjustments to the estimated doublet threshold based on total input cell numbers.

**Sample merge and integration.** To generate the AIH liver atlas, we aggregated ten CITE-seq and six snRNA-seq samples using Seurat's *merge* function. After creating the merged AIH liver Seurat object, RNA assays were normalized using Seurat's *NormalizeData* function, and highly variable genes were identified with the *FindVariableFeatures* function (method = "vst", nfeatures = 2000) across samples. Integration features were selected using the *SelectIntegrationFeatures* function, followed by batch effect correction across patients using Seurat's integration workflow (*FindIntegrationAnchors* and *IntegrateData* function). For the combined analysis of AIH liver and paired blood T cells from patients AIH9, AIH13, and AIH15, we selected T cell clusters identified in the AIH liver atlas and merged them with the corresponding blood CD3<sup>+</sup> samples using the *merge* function. Integration and batch correction were performed using the same approach described above.

**Dimensionality reduction, clustering and cluster annotation.** For each integrated object, the integrated matrix was scaled using the *ScaleData* function with default parameters. Principal component analysis (PCA) was then performed on the scaled data using the *RunPCA* function (npcs = 30), followed by dimensionality reduction with the Uniform Manifold Approximation and Projection (UMAP) method (*RunUMAP* function, dims = 1:30). Using the top 30 principal components, a k-nearest neighbor graph was computed based on Euclidean distances (*FindNeighbors* function). Cell clusters were generated using the *FindClusters* function, adjusting the resolution parameter to the highest value that maintained clear distinctions between adjacent clusters. Next, we normalized scRNA-seq data using Seurat's LogNormalize method and CITE-seq counts using the CLR method. The top differentially expressed genes (DEGs) in each cluster were identified using the *FindAllMarkers* function with parameters min.pct = 0.25 and logfc.threshold = 0.5, employing Wilcoxon rank-sum tests. The *DoHeatmap* function in Seurat was used to visualize the expression of the top marker genes for each cluster. Cluster annotation was performed by matching DEGs with published literature and further validated using EnrichR<sup>6</sup> when necessary. Some clusters (e.g., UD-1) were left undefined due to their heterogeneous gene expression profiles spanning multiple cell types.

UD-2 could be classified as plasmacytoid dendritic cells based on the expression of marker genes such as *PLD4*, *JCHAIN*, and *LILRA4*; however, due to the low number of cells, we opted to annotate them as UD-2. For DEGs, see research data repository under DOI 10.25592/uhhfdm.18135.

**Liver CD4<sup>+</sup> T cells, CD8<sup>+</sup> T cells and hepatocytes clustering.** For the separate analysis of liver CD4<sup>+</sup> T cells, CD8<sup>+</sup> T cells, and hepatocytes, the corresponding clusters identified in the AIH liver atlas were selected and re-integrated by patient. For DEGs, see research data repository under DOI 10.25592/uhhfdm.18135.

Regarding T cells, CD4<sup>+</sup> and CD8<sup>+</sup> T cells were initially re-integrated and re-clustered together to generate a CD3<sup>+</sup> UMAP. Cells were then assigned to the CD4<sup>+</sup> UMAP based on the average *CD4* expression per cluster, while all other cells expressing *CD8A* or belonging to CD8<sup>+</sup> clusters were assigned to the CD8<sup>+</sup> UMAP. CD4<sup>+</sup> and CD8<sup>+</sup> T cells were subsequently re-integrated and re-clustered separately using the previously described method. Detailed cell type annotations were then obtained by examining the top marker genes and CITE-seq expression profiles of the clusters.

For CD4<sup>+</sup> T cell clustering, one donor from CITE-seq and one donor from snRNA-seq were excluded due to low cell numbers (< 80 cells), which affected integration quality. Additionally, since the original cluster 2 of CD4<sup>+</sup> T cells appeared to contain two distinct populations of cells - i.e., one expressing higher level of *IL10* than the other - it was further analysed using Seurat's *FindSubCluster* function and subsequently split into two additional CD4<sup>+</sup> T cell clusters (T<sub>EM-b</sub> and T<sub>EM-e</sub>).

A subset of *CD8A*-expressing cells, originally part of cluster 1 in the CD3<sup>+</sup> UMAP (a CD4<sup>+</sup> cluster), formed a distinct cluster in the CD8<sup>+</sup> UMAP, which was designated as T<sub>CM-b</sub>.

**Processing of TCR-seq data and integration.** TCR-seq data for each sample were processed using Cell Ranger software with the cellranger *vdj* command and the reference genome (vdj\_GRCh38\_alts\_ensembl-5.0.0). The output file *filtered\_contig\_annotations.csv* contained information on TCR- $\alpha$  and TCR- $\beta$  chain CDR3 nucleotide sequences for single cells identified by barcodes. The R package *scRepertoire* was used to combine contig annotation data from different samples into a single list object using the *combineTCR* function. This combined TCR contig list was then integrated with the corresponding Seurat object from CITE-seq data using the *combineExpression* function (*cloneCall* = "gene+nt"). Only cells with both TCR and CITE-seq data were retained for downstream clonotype analysis.

Each cell's clone was defined based on the corresponding amino acid sequence of the CDR3 region. The frequency of each clone (*n*) within each patient was calculated, and the clonotype was categorized by frequency into four groups: single, small, medium, and high.

**Liver and Blood TCR analysis.** To analyse TCR repertoires between the liver and paired blood samples, we generated a UMAP combining liver CD4<sup>+</sup> and CD8<sup>+</sup> T cells alongside blood sample CD3<sup>+</sup> T cells. To balance cell numbers and capture full transcriptional diversity from liver and blood, the UMAP was generated using all liver donors and three paired blood samples. Subsequently, liver cells from the three donors with paired blood samples were used for further TCR analysis.

We compared and quantified clonotypes between either liver CD4<sup>+</sup> or liver CD8<sup>+</sup> T cells, and their paired blood CD3<sup>+</sup> T cells. In particular, we highlighted the clones shared between the liver and blood compartments, as well as liver-specific clones, in the CD4<sup>+</sup> and CD8<sup>+</sup> liver UMAPs.

In the liver TCR analysis of CD4<sup>+</sup> T cells, 14 clones from 3 clonotypes shared between liver and blood were not present in the CD4<sup>+</sup> T cell UMAP, as they clustered within CD8<sup>+</sup> T cell UMAP. Notably, only 3 of the 14 excluded shared clones exhibited a gene signature similar to that of T<sub>RM</sub>1 cells. For the same reason, 6 clones from 3 liver-specific clonotypes were not present in the CD4<sup>+</sup> UMAP and 2 of these 6 clones exhibited a gene signature similar to that of T<sub>RM</sub>1 cells.

**Calculation of gene signature scores.** Signature scores for gene sets were calculated using Seurat's *AddModuleScore* function with default parameters. The residency and migration gene sets for CD4<sup>+</sup> and CD8<sup>+</sup> T cells were derived from published ~~core~~ lists of core genes upregulated in CD69<sup>+</sup> CD4<sup>+</sup> and CD69<sup>+</sup> CD8<sup>+</sup> T cells, respectively (Table S8), whereas migratory gene sets were derived from lists of core genes upregulated in CD69<sup>-</sup> CD4<sup>+</sup> and CD69<sup>-</sup> CD8<sup>+</sup> T cell (Table S9)<sup>7</sup> The a.a. gene set consisted of a core list of upregulated genes identified in a.a. CD8<sup>+</sup> T cells from human NASH liver (Table S10).<sup>8</sup> We used the *lme* function (*nlme* package) to apply a linear mixed-effects model with the patient ID as a random effect. We applied a Dunnett's test post-hoc, comparing each T<sub>EM</sub> cluster to the pool of the two TCM clusters, using the *glht* function (*multcomp* package).

**Interactome Analysis.** The R package CellChat<sup>9</sup> and its associated database were utilized to calculate the interaction strength. Based on the results from our bulk mRNA sequencing analysis, we used a supervised approach to select only the ligands *TNF*, *IFNG*, *FASLG*, *IL7*, and *IL15* from CellChat's database. Additionally, we integrate the *IL15 trans* presentation<sup>10</sup> into the database, specifying the following interaction: (*IL15 + IL15RA*) - (*IL2RG + IL2RB*). The communication probability was determined using the *computeCommunProb* method, with the truncated mean approach and a trim factor set to 0.05. To visualize the interaction network, we used the R package *ggraph*.

**Regression of TNF-dependent adhesive molecules on hepatocytes.** The R package AUCell was used to calculate the TNF pathway score and thresholds in hepatocytes based on the annotated genes of the KEGG TNF Pathway (hsa04668), excluding genes annotated in the KEGG Cell Adhesion Molecules pathway (hsa04514). Given the sparsity of the snRNA-sequencing data, we performed a zero-inflated regression using a hurdle model to estimate the relationship between the calculated TNF score and cell adhesion molecule expression. For this, we used the *zlm* method from the R package MAST, correcting for feature counts and sample identity.

### **Xenium *in situ* spatial analysis workflow**

**Gene panel design.** The Xenium In Situ technology used targeted panels to detect gene expression, including 377 genes from the Xenium Human Multi-Tissue and Cancer Panel (10X Genomics) and an additional 100 custom genes (10X Genomics) selected based on CITE-seq and snRNA-seq data from human AIH liver tissue.

**Xenium data generation.** The Xenium workflow began with sectioning 5µm FFPE tissue onto a Xenium slide, following the Xenium In Situ for FFPE - Tissue Preparation Guide (10X Genomics, CG000578). Deparaffinization and permeabilization were then performed to make the mRNA accessible, using the Xenium In Situ for FFPE - Deparaffinization & Decrosslinking Demonstrated Protocol (10X Genomics, CG000580). The mRNAs were targeted by the 477 probes described earlier, following the Xenium In Situ Gene Expression - Probe Hybridization, Ligation, Amplification & Cell Segmentation User Guide (10X Genomics, CG000749). Subsequently, slides were loaded onto the automated Xenium Analyzer (10X Genomics, GC000584). Regions of interest covering the full tissue sections were selected for imaging and processed using the fully automated, on-instrument analysis pipeline in Xenium Analyzer software (v3.0).

**Pre-processing of Xenium data and integration.** Xenium data was analysed in R, using Seurat and tidyverse packages. Data from the Xenium Onboard Analysis was imported into Seurat for each sample, filtering out cells without any RNA signals. To identify cell types, RNA count tables from all AIH and all control samples were merged separately, normalized using *SCTransform* function and integrated using Harmony (15 iterations, no early stop). UMAP and (shared) nearest-neighbour graphs were calculated using the first 30 harmony-adjusted embeddings. Cells were clustered using the Louvain algorithm at resolution 0.4 and annotated based on marker gene expression. As specified in the legend to Fig.4d, we identified T<sub>RM</sub>1

cells as CD4<sup>+</sup> T cells that express *CD69* and/or *CXCR6* in combination with *TNF* and/or *IFNG*; a.a.CD8<sup>+</sup> T cells were defined within the CD8<sup>+</sup> T cell cluster as CD69<sup>-</sup> CD62L<sup>-</sup> CCR7<sup>-</sup>.

**Spatial cell-cell communication analysis.** CellChat was used to calculate interaction probabilities as described above for the CITE-seq and snRNA-seq data, but additionally using an interaction range of 50 µm for soluble ligands and 10 µm for contact dependent interactions.

**Spatial neighbourhood analysis.** The *get.knnx* function from the FNN package was used to calculate the 5 nearest neighbouring cells around each cell in each sample. For each sample and cell type, neighbours were tallied by cell type and quantified as proportion of total neighbouring cells.

**TNF reacting cell analysis.** The distance to the closest TNF producing cells was calculated for each cell in each sample. For cells within 20 µm of a TNF producing cell, TNF-receptor positive and TNF-receptor negative cells were compared using the *FindMarkers* function, applying a Wilcoxon Rank Sum test followed by Bonferroni correction for multiple hypothesis testing. TNF-receptor positive was defined as the expression of either *TNFRSF1A* or *TNFRSF1B*.

### **Statistical analyses**

Statistical analyses were performed using R and GraphPad Prism. The statistical tests applied to each dataset were described in the corresponding figure legends. Patients from the clinical trial receiving infliximab (n=12) were matched to patients from the R-LIVER registry receiving standard care (SoC, n=24). in a 1:2 ratio using propensity score matching (PSM). Propensity scores were estimated via logistic regression including the baseline covariates age, ALT, mHAI, bilirubin and IgG, while sex and histological evidence of advanced fibrosis/cirrhosis (F3/4) were included as exact matching variables (see Fig. S10b-c for details of the PSM). Given the high collinearity between AST and ALT in the dataset (see Fig. S10a), AST was not included in the Propensity Matching to avoid redundancy-related overfitting of the model. Matching was performed without replacement using the nearest-neighbour method with an ATT (average treatment effect on the treated) estimate. Covariate balance was assessed using standardized mean differences (SMDs), with values <0.2 considered sufficiently balanced. After matching, all covariates achieved this threshold, with the exception of AST (SMD = 0.96); to account for this residual imbalance, AST was hence included as a covariate in subsequent analyses to adjust for residual confounding. Baseline variables of patients in the IFX and the SoC cohort were summarized descriptively, group comparability was assessed using SMDs (Table 1). Group comparisons for AST, ALT, IgG, liver stiffness (LSM) and Body Mass Index

(BMI) were performed by fitting linear mixed-effects models (LMM) to evaluate the effects of group (IFX vs. SoC) and time point (baseline vs month 6) on the respective parameters. To account for subject-level variability, all models included a random intercept for each participant and fixed effects for group, time point, and their interaction. Models were estimated using restricted maximum likelihood and t-tests employed Satterthwaite's approximation for degrees of freedom. Within-group changes from baseline to 6 months were assessed using estimated marginal means (EMMs) derived from the fitted models.

### Supplementary references

- 1 Bolger AM, Lohse M, Usadel B. Trimmomatic: a flexible trimmer for Illumina sequence data. *Bioinformatics*. 2014;30:2114-20.
- 2 Love MI, Huber W, Anders S. Moderated estimation of fold change and dispersion for RNA-seq data with DESeq2. *Genome Biology*. 2014;15:550.
- 3 Müller-Dott S, Tsirvouli E, Vazquez M, et al. Expanding the coverage of regulons from high-confidence prior knowledge for accurate estimation of transcription factor activities. *Nucleic Acids Res*. 2023;51:10934-10949.
- 4 Litviňuková M, Talavera-López C, Maatz H, et al. Cells of the adult human heart. *Nature*. 2020;588:466-472.
- 5 Yates AD, Achuthan P, Akanni W, et al. Ensembl 2020. *Nucleic Acids Res*. 2020;48:D682-D688.
- 6 Kuleshov MV, Jones MR, Rouillard AD, et al. Enrichr: a comprehensive gene set enrichment analysis web server 2016 update. *Nucleic Acids Research*. 2016; gkw377
- 7 Kumar BV, Ma W, Miron M, et al. Human Tissue-Resident Memory T Cells Are Defined by Core Transcriptional and Functional Signatures in Lymphoid and Mucosal Sites. *Cell Rep*. 2017;20:2921-2934.
- 8 Dudek M, Pfister D, Donakonda S, et al. Auto-aggressive CXCR6+ CD8 T cells cause liver immune pathology in NASH. *Nature*. 2021;592:444-449.
- 9 Jin S, Plikus MV, Nie Q. CellChat for systematic analysis of cell-cell communication from single-cell transcriptomics. *Nat Protoc*. 2025;20:180-219.
- 10 Jabri B, Abadie V. IL-15 functions as a danger signal to regulate tissue-resident T cells and tissue destruction. *Nat Rev Immunol*. 2015;15:771-83.

## Supplementary tables

**Table S1**

### Journal of Hepatology CTAT methods

Tables for a “Complete, Transparent, Accurate and Timely account” (CTAT) are now mandatory for all revised submissions. The aim is to enhance the reproducibility of methods.

- Only include the parts relevant to your study
- Refer to the CTAT in the main text as ‘Supplementary CTAT Table’
- Do not add subheadings
- Add as many rows as needed to include all information
- Only include one item per row

**If the CTAT form is not relevant to your study, please outline the reasons why:**

|  |
|--|
|  |
|--|

#### 1.1 Antibodies

| Name  | Citation | Supplier       | Cat no.    | Clone no. |
|---|----------|----------------|------------|-----------|
| anti-human CD45 PE-Cy7                                      |          | BioLegend      | 304016     | HI30      |
| anti-human CD3 FITC   |          | BioLegend      | 344804     | SK7       |
| anti-human TCR $\alpha/\beta$ AF488                         |          | BioLegend      | 306712     | IP26      |
| anti-human TCR $\gamma/\delta$ PerCP-Cy5.5                  |          | BioLegend      | 331224     | BI4       |
| anti-human TCR V $\alpha$ 24-J $\alpha$ 18 BV421            |          | BioLegend      | 342916     | 6B11      |
| anti-human CD4 BV605  |          | BioLegend      | 317438     | OKT4      |
| anti-human CD8 $\alpha$ APC-Cy7                             |          | BioLegend      | 300926     | HIT8a     |
| anti-human CD8a BV711                                       |          | BioLegend      | 301044     | RPA-T8    |
| anti-human CD45RO AF700                                     |          | BioLegend      | 304218     | UCHL1     |
| anti-human CD45RO PE/Cy5                                    |          | BioLegend      | 304208     | UCHL1     |
| anti-human CD62L BV421                                      |          | BioLegend      | 304827     | DREG-56   |
| anti-human CD25 BV510                                       |          | BioLegend      | 302639     | BC96      |
| anti-human CD127 PE-Cy7                                     |          | BioLegend      | 351320     | A019D5    |
| anti-human CD69 BV785                                       |          | BioLegend      | 310932     | FN50      |
| anti-human CD69 BV650                                       |          | BioLegend      | 310933     | FN50      |
| anti-human CXCR6 PE/Dazzle                                  |          | BioLegend      | 356016     | K041E5    |
| anti-human CD49a AF647                                      |          | BioLegend      | 328310     | TS2/7     |
| anti-human TIGIT PE   |          | BioLegend      | 372703     | A15153G   |
| anti-human PD-1 BV650                                       |          | BioLegend      | 329950     | EH12.2H7  |
| anti-human TNF AF488  |          | BioLegend      | 502917     | MaAb11    |
| anti-human IFN- $\gamma$ BV785                              |          | BioLegend      | 502542     | 4S.B3     |
| anti-human Granzyme A PE-Cy7                                |          | BioLegend      | 507221     | CB9       |
| anti-human Granzyme B BV510                                 |          | BD Biosciences | 563388     | GB11      |
| anti-human Granzyme K PE                                    |          | BioLegend      | 370511     | GM26E7    |
| Phospho-STAT5 Monoclonal Antibody, PE                       |          | Thermo Fisher  | 12-9010-42 | SRBCZX    |
| TotalSeq <sup>TM</sup> -C Human Universal Cocktail V 1.0    |          | BioLegend      | 399905     | --        |
| TotalSeq <sup>TM</sup> -C0048 anti-human CD45               |          | BioLegend      | 368545     | 2D1       |
| TotalSeq <sup>TM</sup> -C0224 anti-human TCR $\alpha/\beta$ |          | BioLegend      | 306743     | IP26      |
| TotalSeq <sup>TM</sup> -C0045 anti-human CD4                |          | BioLegend      | 344651     | SK3       |

|                                   |  |           |         |            |
|-----------------------------------|--|-----------|---------|------------|
| TotalSeq™-C0046 anti-human CD8    |  | BioLegend | 344753  | SK1        |
| TotalSeq™-C0085 anti-human CD25   |  | BioLegend | 302649  | BC96       |
| TotalSeq™-C0390 anti-human CD127  |  | BioLegend | 351356  | A019D5     |
| TotalSeq™-C0146 anti-human CD69   |  | BioLegend | 310951  | FN50       |
| TotalSeq™-C0145 anti-human CD103  |  | BioLegend | 350233  | Ber-ACT8   |
| TotalSeq™-C0140 anti-human CXCR3  |  | BioLegend | 353747  | G025H7     |
| TotalSeq™-C0143 anti-human CCR6   |  | BioLegend | 353440  | G034E3     |
| TotalSeq™-C0148 anti-human CCR7   |  | BioLegend | 353251  | G043H7     |
| TotalSeq™-C0169 anti-human TIM-3  |  | BioLegend | 345049  | F38-2E2    |
| TotalSeq™-C0152 anti-human LAG-3  |  | BioLegend | 369335  | 11C3C65    |
| TotalSeq™-C0371 anti-human CD49b  |  | BioLegend | 359317  | P1E6-C5    |
| TotalSeq™-C0088 anti-human PD-1   |  | BioLegend | 329963  | EH12.2H7   |
| TotalSeq™-C0151 anti-human CTLA-4 |  | BioLegend | 369621  | BNI3       |
| Anti-CD71 antibody                |  | BioLegend | 334102  | CY1G4      |
| Anti-TNF neutralizing antibody    |  | BioXcell  | SIM0001 | Adalimumab |

## 1.2 Cell lines

| Name | Citation | Supplier | Cat no.  | Passage no. | Authentication test method |
|------|----------|----------|----------|-------------|----------------------------|
| K562 |          | ATCC     | CCL-243™ |             |                            |

## 1.3 Organisms

| Name | Citation | Supplier | Strain | Sex | Age | Overall n number |
|------|----------|----------|--------|-----|-----|------------------|
|      |          |          |        |     |     |                  |

## 1.4 Sequence based reagents

| Name   | Sequence  | Supplier                 |
|--|---|--------------------------|
| TaqMan probes:<br>TNF<br>IFNG<br>IL12A<br>IL1B<br>HPRT | Hs01113624_g1<br>Hs00989291_m1<br>Hs01073447_m1<br>Hs01555410_m1<br>Hs02800695_m1 | Thermo Fisher Scientific |
| Chromium Next GEM Single Cell V(D)J Reagent Kits v1.1  |   | 10X Genomics             |
| Chromium Next GEM Single Cell 3' Reagent Kits v3.1     |   | 10x Genomics             |
| Xenium In Situ Gene Expression Kit                     |   | 10x Genomics             |

## 1.5 Biological samples

| Description           | Source | Identifier |
|-----------------------|--------|------------|
| Liver biopsies        | human  |            |
| Primary blood T cells | human  |            |
| Primary hepatocytes   | human  |            |

## 1.6 Deposited data

| Name of repository | Identifier | Link |
|--------------------|------------|------|
|                    |            |      |

|  |  |  |
|--|--|--|
|  |  |  |
|--|--|--|

## 1.7 Software

| Software name   | Manufacturer  | Version                             |
|-----------------|---|-------------------------------------|
| RStudio         | Posit Software, PBC formerly RStudio, PBC<br>Boston, MA, USA  | 2023.12.1+402<br>"Ocean Storm"      |
| Biorender       | Science Suite Inc.  | Version 2025                        |
| CellRanger      | 10X Genomics  | 6.1.1                               |
| Trimmomatic     | Usadel Lab (RWTH Aachen University)   | 0.36                                |
| FastQC          | Babraham Bioinformatics (Babraham Institute)  | 0.11.5                              |
| STAR            | Dobin Lab (Cold Spring Harbor Laboratory)   | 2.7.3a                              |
| R               | R Foundation for Statistical Computing  | 4.3.3                               |
| Seurat          | Satija Lab <a href="https://github.com/satijalab/seurat">https://github.com/satijalab/seurat</a>  | 4.3.0 (SCS/SNS) /<br>5.0.3 (Xenium) |
| DoubletFinder   | Chris McGinnis (UCSF)<br><a href="https://github.com/chris-mcginnis-ucsf/DoubletFinder">https://github.com/chris-mcginnis-ucsf/DoubletFinder</a>          | 2.0.3                               |
| scRepertoire    | Nick Borcharding (Borcharding Lab)<br><a href="https://github.com/BorchLab/scRepertoire">https://github.com/BorchLab/scRepertoire</a>                     | 1.12.0                              |
| CellChat        | Suoqin Jin<br><a href="https://github.com/jinworks/CellChat">https://github.com/jinworks/CellChat</a>   | 2.1.2                               |
| tidyverse       | Posit Software<br><a href="https://cran.r-project.org/web/packages/tidyverse/index.html">https://cran.r-project.org/web/packages/tidyverse/index.html</a> | 2.0.0                               |
| Harmony         | Ilya Korsunsky (Raychaudhuri Lab)<br><a href="https://github.com/immunogenomics/harmony">https://github.com/immunogenomics/harmony</a>                    | 1.2.0                               |
| FNN             | Shengqiao Li<br><a href="https://cran.r-project.org/web/packages/FNN/index.html">https://cran.r-project.org/web/packages/FNN/index.html</a>               | 1.1.14                              |
| nlme            | R Core Team<br><a href="https://cran.r-project.org/web/packages/nlme/index.html">https://cran.r-project.org/web/packages/nlme/index.html</a>              | 3.1                                 |
| multcomp        | Torsten Hothorn<br><a href="https://cran.r-project.org/web/packages/multcomp/index.html">https://cran.r-project.org/web/packages/multcomp/index.html</a>  | 1.4                                 |
| org.Hs.eg.db    | Bioconductor Core Team<br><a href="https://bioconductor.org/packages/org.Hs.eg.db/">https://bioconductor.org/packages/org.Hs.eg.db/</a>                   | 3.19.1                              |
| KEGGREST        | Bioconductor Core Team<br><a href="https://bioconductor.org/packages/KEGGREST/">https://bioconductor.org/packages/KEGGREST/</a>                           | 1.44.1                              |
| clusterProfiler | Guangchuang Yu<br><a href="https://bioconductor.org/packages/clusterProfiler/">https://bioconductor.org/packages/clusterProfiler/</a>                     | 4.12.2                              |
| DESeq2          | Michael Love<br><a href="https://bioconductor.org/packages/DESeq2">https://bioconductor.org/packages/DESeq2</a>   | 1.44.0                              |
| vegan           | Jari Oksanen / vegandevs<br><a href="https://cran.r-project.org/package=vegan">https://cran.r-project.org/package=vegan</a>                               | 2.6-8                               |
| decoupleR       | Pau Badia-i-Mompel (Saez-Rodriguez Lab)<br><a href="https://github.com/saezlab/decoupleR">https://github.com/saezlab/decoupleR</a>                        | 2.10.0                              |
| fgsea           | Alexey Sergushichev<br><a href="https://bioconductor.org/packages/fgsea">https://bioconductor.org/packages/fgsea</a>                                      | 1.28.0                              |
| dplyr           | Posit / Tidyverse Team<br><a href="https://cran.r-project.org/package=dplyr">https://cran.r-project.org/package=dplyr</a>                                 | 1.1.4                               |
| ggplot2         | Posit / Tidyverse Team<br><a href="https://cran.r-project.org/package=ggplot2">https://cran.r-project.org/package=ggplot2</a>                             | 3.5.1                               |

|           |  |        |
|-----------|--|--------|
| ggvoronoi | Robert C. Garrett<br><a href="https://github.com/garrettc/ggvoronoi">https://github.com/garrettc/ggvoronoi</a>                     | 0.8.6  |
| ggpubr    | Alboukadel Kassambara<br><a href="https://github.com/kassambara/ggpubr/releases">https://github.com/kassambara/ggpubr/releases</a> | 0.6.0  |
| ggpmisc   | Pedro J. Aphalo<br><a href="https://github.com/aphalo/ggpmisc">https://github.com/aphalo/ggpmisc</a>                               | 0.6.0  |
| ggrepel   | Kamil Slowikowski<br><a href="https://github.com/slowkow/ggrepel">https://github.com/slowkow/ggrepel</a>                           | 0.9.5  |
| ggraph    | Thomas Lin Pedersen<br><a href="https://github.com/thomasp85/ggraph">https://github.com/thomasp85/ggraph</a>                       | 2.2.1  |
| stringr   | Posit / Tidyverse Team<br><a href="https://github.com/tidyverse/stringr">https://github.com/tidyverse/stringr</a>                  | 1.5.1  |
| reshape2  | Hadley Wickham<br><a href="https://cran.r-project.org/package=reshape2">https://cran.r-project.org/package=reshape2</a>            | 1.4.4  |
| AUCell    | Gert Hulselmans (Aerts Lab)<br><a href="https://github.com/aertslab/AUCell">https://github.com/aertslab/AUCell</a>                 | 1.26.0 |
| MAST      | Andrew McDavid (Gottardo Lab)<br><a href="https://github.com/RGLab/MAST">https://github.com/RGLab/MAST</a>                         | 1.30.0 |

### 1.8 Other (e.g. drugs, proteins, vectors etc.)

|  |                    |             |
|--|--------------------|-------------|
| NucleoSpin RNA Kit                               | Macherey-Nagel     |             |
| High-Capacity cDNA Reverse Transcription Kit     | Thermo Fisher      |             |
| KAPA PROBE FAST Universal 2X qPCR Master Mix Kit | Roche              |             |
| High Sensitivity DNA Kit                         | Agilent            | 5067-4626   |
| DPBS   | Gibco              | 14190-094   |
| EDTA   | Sigma-Aldrich      | 03690       |
| Collagenase D                                    | Roche              | 11088882001 |
| DNase I  | Roche              | 10104159001 |
| Fixable Viability Dye eFluor 506                 | Thermo Fisher      | 65-0866-14  |
| Zombie UV Fixable Viability Kit                  | BioLegend          | 423108      |
| Alexa Fluor 750 NHS Ester                        | Thermo Fisher      | A20011      |
| Human FC Block                                   | BD Biosciences     | 564220      |
| Phorbol-12-myristate-13-acetate (PMA)            | Sigma-Aldrich      | 524400      |
| Ionomycin from Streptomyces conglobatus          | Sigma-Aldrich      | I9657       |
| Brefeldin A Solution (1,000X)                    | BioLegend          | 420601      |
| BD Cytotfix/Cytoperm™ Plus                       | BD Biosciences     | 555028      |
| Lectin from Phaseolus vulgaris (PHA)             | Sigma-Aldrich      | L9017       |
| Recombinant human IL-2                           | Miltenyi Biotec    | 130-097-746 |
| Recombinant human IL-7                           | R&D system         | 207-IL/CF   |
| Recombinant human IL-15                          | R&D system         | 247-ILB/CF  |
| Recombinant human IL-15                          | PeproTech          | AF-200-15   |
| Recombinant human TNF                            | PeproTech          | 300-01A     |
| Ficoll-Paque PLUS                                | Cytiva             | 17144003    |
| Pancoll  | PAN Biotech        | P04-60100   |
| FBS Supreme                                      | PAN Biotech        | P30-3031    |
| RPMI Medium 1640, GlutaMAX™                      | Gibco              | 61870-010   |
| X-VIVO medium                                    | Lonza              | 02-060F     |
| Collagen R                                       | Advanced Biomatrix | 5026        |
| Williams E medium                                | Gibco              | 22551-022   |
| Insulin-transferrin-selenium                     | Gibco              | 41400-045   |
| Bovine Serum Albumin                             | AppliChem          | A1391,0500  |
| GlutaMAX   | Sigma-Aldrich      | G7513       |

|   |                       |                |
|---|-----------------------|----------------|
| Non-essential amino acids   | Gibco                 | 11140-035      |
| Penicillin-Streptomycin   | Sigma-Aldrich         | P0781          |
| CD8 MicroBeads, human   | Miltenyi Biotec       | 130-045-201    |
| CellTrace CFSE cell proliferation kit                                     | Thermo Fisher         | C34554         |
| CellTrace Violet cell proliferation kit                                   | Thermo Fisher         | C34557         |
| Dynabeads™ Human T-Activator CD3/CD28 for T Cell Expansion and Activation | Gibco                 | 11161D         |
| ImmunoCult Human CD3/CD28 T Cell Activator                                | STEMCELL Technologies | 10971          |
| LEGENDplex Human CD8/NK Panel   | BioLegend             | 741148         |
| Infliximab (Inflectra®)   | Pfizer                | Not applicable |
|   |                       |                |

**1.9 Please provide the details of the corresponding methods author for the manuscript:**

|  |
|--|
|  |
|--|

**2.0 Please confirm for randomised controlled trials all versions of the clinical protocol are included in the submission. These will be published online as supplementary information.**

|   |
|---|
| <p>The phase IIa clinical trial (EudraCT No.: 2017-003311-19) followed a proof-of-concept design and was therefore not randomised nor controlled. To ensure maximum transparency, the most recent version of the protocol (V3.0) has been added to the supplementary material provided.</p> |
|---|

**Table S2. Comparison of biochemical markers, liver stiffness and BMI during baseline and after 6 months between patients receiving IFX and the cohort receiving the standard of care (SoC) for 6 months.**

|                                | IFX                           |                  |                 | SoC                           |                               |                 |
|--------------------------------|-------------------------------|------------------|-----------------|-------------------------------|-------------------------------|-----------------|
|                                | Baseline (FA)                 | Week 24 (FA)     | Relative Change | Baseline                      | Month 6                       | Relative Change |
| <b>AST xULN</b>                | 6.48 (3.32-16.71)             | 0.71 (0.29-1.66) | -89.0%          | 16.49 (4.26-28.46)            | 1.01 (0.42-10.12)             | -93.9%          |
| <b>ALT xULN</b>                | 11.29 (4.4-21.54)             | 0.83 (0.31-1.97) | -92.7%          | 13.11 (2.16-24.26)            | 0.81 (0.34-3.62)              | -93.8%          |
| <b>IgG (g/l)</b>               | 19.4 (14.3-32.1)              | 16.7 (12.7-25.2) | -13.2%          | 19.8 (1.8-51.2)               | 11.7 (1.3-30.9)               | -40.9%          |
| <b>gGT (U/l)</b>               | 116 (41-331)                  | 35 (9-93)        | -69.8%          | 146 (50-422)                  | 36 (11-352)                   | -75.3%          |
| <b>ALP (U/l)</b>               | 131 (67-343)                  | 73 (48-150)      | -44.3%          | 130 (59-396)                  | 66 (41-149)                   | -49.2%          |
| <b>Total Bilirubin (mg/dl)</b> | 1.1 (0.5-4.7)                 | 0.6 (0.3-1.4)    | -45.5%          | 1.2 (0.4-3.0)                 | 0.7 (0.3-1.3)                 | -41.7%          |
| <b>Albumin (g/dl)</b>          | 35.7 (33.0-41.7) <sup>1</sup> | 42.8 (37.9-45.4) | +19.9%          | 37.0 (25.6-46.1) <sup>3</sup> | 41.3 (29.8-45.8) <sup>3</sup> | +11.6%          |
| <b>INR</b>                     | 1.0 (1.0-1.1) <sup>2</sup>    | 1.0 (0.9-1.1)    | ±0.0%           | 1.1 (0.9-1.5)                 | 1.0 (0.9-1.2) <sup>3</sup>    | -9.1%           |
| <b>Liver stiffness (kPa)</b>   | 14.8 (6.9-34.8)               | 7.1 (5.2-18.8)   | -52.0%          | 10.4 (4.9-35.3) <sup>4</sup>  | 7.0 (3.5-22.3) <sup>5</sup>   | -32.7%          |
| <b>BMI (kg/m<sup>2</sup>)</b>  | 25.1 (19.2-32.1)              | 25.5 (19.5-32.4) | +1.6%           | 23.7 (17.9-33.5) <sup>6</sup> | 25.5 (21.2-32.0) <sup>7</sup> | +7.6%           |

Shown are data of patients with values **both at baseline and at month 6** (IFX [final analysis, FA] cohort n = 9, SoC cohort n = 24, if not specified differently).

Continuous variables = medians (range)

<sup>1</sup> data available for n = 6

<sup>2</sup> data available for n = 7

<sup>3</sup> data available for n = 22

<sup>4</sup> data available for n = 18

<sup>5</sup> data available for n = 13

<sup>6</sup> data available for n = 23

<sup>7</sup> data available for n = 15

**Table S3. Results of the Short Form 36 questionnaire (SF-36) regarding health-related quality of life from patients in the clinical trial.**

| Baseline  | ID 001        | ID 002        | ID 003        | ID 004        | ID 005        | ID 006        | ID 007        | ID 008        | ID 009        | ID 011        | ID 012        | ID 013        | Median        | Mean        | SD        | IQR25        | IQR75        | Min        | Max        |
|---|---------------|---------------|---------------|---------------|---------------|---------------|---------------|---------------|---------------|---------------|---------------|---------------|---------------|-------------|-----------|--------------|--------------|------------|------------|
| Physical Function                                       | 80            | 80            | 80            | 55            | 85            | 85            | 85            | 70            | 35            | 85            | 80            | 80            | 80,0          | 75,0        | 14,6      | 77,5         | 85,0         | 35         | 85         |
| Mental Health   | 88            | 60            | 92            | 92            | 84            | 68            | 80            | 56            | 64            | 76            | 80            | 84            | 80,0          | 77,0        | 11,8      | 67,0         | 85,0         | 56         | 92         |
| Pain  | 89            | 100           | 100           | 44            | 56            | 89            | 100           | 100           | 78            | 78            | 100           | 89            | 89,0          | 85,3        | 17,8      | 78,0         | 100,0        | 44         | 100        |
| Change in Health  | 25            | 25            | 50            | 25            | 25            | 25            | 25            | 0             | 0             | 75            | 50            | 25            | 25,0          | 29,2        | 20,0      | 25,0         | 31,3         | 0          | 75         |
| Role limitation physical                                | 75            | 50            | 100           | 100           | 50            | 100           | 100           | 0             | 0             | 100           | 100           | 50            | 87,5          | 68,8        | 37,0      | 50,0         | 100,0        | 0          | 100        |
| Role limitation emotional                               | 100           | 67            | 100           | 100           | 100           | 67            | 100           | 0             | 0             | 100           | 100           | 100           | 100,0         | 77,8        | 36,8      | 67,0         | 100,0        | 0          | 100        |
| Energy/Vitality   | 70            | 25            | 75            | 50            | 45            | 55            | 65            | 0             | 30            | 45            | 70            | 20            | 47,5          | 45,8        | 22,3      | 28,8         | 66,3         | 0          | 75         |
| Health Perception                                       | 70            | 50            | 65            | 50            | 90            | 75            | 75            | 0             | 50            | 45            | 80            | 30            | 57,5          | 56,7        | 23,7      | 48,8         | 75,0         | 0          | 90         |
| <b>6 Months</b>   | <b>ID 001</b> | <b>ID 002</b> | <b>ID 003</b> | <b>ID 004</b> | <b>ID 005</b> | <b>ID 006</b> | <b>ID 007</b> | <b>ID 008</b> | <b>ID 009</b> | <b>ID 011</b> | <b>ID 012</b> | <b>ID 013</b> | <b>Median</b> | <b>Mean</b> | <b>SD</b> | <b>IQR25</b> | <b>IQR75</b> | <b>Min</b> | <b>Max</b> |
| Physical Function                                       | 85            | 80            | 80            | 65            | 85            | 85            | 85            |               |               | 85            | 85            | 85            | 85,0          | 81,7        | 6,2       | 80,0         | 85,0         | 65         | 85         |
| Mental Health   | 92            | 68            | 92            | 92            | 80            | 44            | 88            |               |               | 88            | 92            | 64            | 88,0          | 79,1        | 16,1      | 68,0         | 92,0         | 44         | 92         |
| Pain  | 89            | 100           | 89            | 89            | 100           | 67            |               |               |               | 100           | 100           | 100           | 100,0         | 92,7        | 10,4      | 89,0         | 100,0        | 67         | 100        |
| Change in Health  | 75            | 75            | 75            | 100           | 25            | 50            |               |               |               | 75            | 50            | 75            | 75,0          | 66,7        | 20,4      | 50,0         | 75,0         | 25         | 100        |
| Role limitation physical                                | 100           | 100           | 100           | 100           | 100           | 50            |               |               |               | 100           | 100           | 100           | 100,0         | 94,4        | 15,7      | 100,0        | 100,0        | 50         | 100        |
| Role limitation emotional                               | 100           | 100           | 100           | 100           | 67            | 0             |               |               |               | 100           | 100           | 33            | 100,0         | 77,8        | 35,2      | 67,0         | 100,0        | 0          | 100        |
| Energy/Vitality   | 75            | 60            | 75            | 75            | 60            | 35            |               |               |               | 60            | 75            | 60            | 60,0          | 63,9        | 12,4      | 60,0         | 75,0         | 35         | 75         |
| Health Perception                                       | 85            | 75            | 70            | 65            | 65            | 55            |               |               |               | 70            | 75            | 70            | 70,0          | 70,0        | 7,8       | 65,0         | 75,0         | 55         | 85         |
| <b>Differences (A<sub>6</sub> results vs. Baseline)</b> | <b>ID 001</b> | <b>ID 002</b> | <b>ID 003</b> | <b>ID 004</b> | <b>ID 005</b> | <b>ID 006</b> | <b>ID 007</b> | <b>ID 008</b> | <b>ID 009</b> | <b>ID 011</b> | <b>ID 012</b> | <b>ID 013</b> | <b>Median</b> | <b>Mean</b> | <b>SD</b> | <b>IQR25</b> | <b>IQR75</b> | <b>Min</b> | <b>Max</b> |
| Physical Function                                       | 5             | 0             | 0             | 10            | 0             | 0             | 0             |               |               | 0             | 5             | 5             | 0,0           | 2,8         | 3,4       | 0,0          | 5,0          | 0          | 10         |
| Mental Health   | 4             | 8             | 0             | 0             | 12            | -36           |               |               |               | 12            | 12            | -20           | 4,0           | -0,9        | 15,6      | 0,0          | 12,0         | -36        | 12         |
| Pain  | 0             | 0             | -11           | 45            | 11            | -33           |               |               |               | 22            | 0             | 11            | 0,0           | 5,0         | 20,4      | 0,0          | 11,0         | -33        | 45         |
| Change in Health  | 50            | 50            | 25            | 75            | 0             | 25            |               |               |               | 0             | 0             | 50            | 25,0          | 30,6        | 25,8      | 0,0          | 50,0         | 0          | 75         |
| Role limitation physical                                | 25            | 50            | 0             | 0             | 0             | -50           |               |               |               | 0             | 0             | 50            | 0,0           | 8,3         | 28,9      | 0,0          | 25,0         | -50        | 50         |
| Role limitation emotional                               | 0             | 33            | 0             | 0             | 0             | -100          |               |               |               | 0             | 0             | -67           | 0,0           | -14,9       | 38,8      | 0,0          | 0,0          | -100       | 33         |
| Energy/Vitality   | 5             | 35            | 0             | 25            | 5             | -30           |               |               |               | 15            | 5             | 40            | 5,0           | 11,1        | 19,8      | 5,0          | 25,0         | -30        | 40         |
| Health Perception                                       | 15            | 25            | 5             | 15            | -10           | -20           |               |               |               | 25            | -5            | 40            | 15,0          | 10,0        | 18,1      | -5,0         | 25,0         | -20        | 40         |

Follow-up data is missing for n = 3 patients who were not eligible for endpoint analysis due to early treatment discontinuation.

**Table S4. Clinical characteristics of bulk mRNA-seq cohorts.**

|                              | Autoimmune hepatitis | Primary biliary cholangitis | p                     |
|------------------------------|----------------------|-----------------------------|-----------------------|
|                              | N=16                 | N=11                        |                       |
| <b>Basic characteristics</b> |                      |                             |                       |
| Age - median (range)         | 51 (25 - 70)         | 53.5 (40 - 82)              | 0.256*                |
| Sex Female – no (%)          | 10 (62.5%)           | 9 (81.8%)                   | 0.404**               |
| <b>Histological features</b> |                      |                             |                       |
| mHAI Score                   |                      |                             |                       |
| Median (range) (missing)     | 9 (4-14) (0)         | 4 (1-8) (0)                 | 0.002*                |
| <6 – no (%)                  | 5 (31.2)             | 8 (72.7)                    |                       |
| 6-9 – no (%)                 | 3 (29.8)             | 3 (27.3)                    |                       |
| 10-18 – no (%)               | 8 (50.0)             | 0 (0)                       |                       |
| Fibrosis score               |                      |                             |                       |
| Median (range) (missing)     | 2 (0-4) (0)          | 2 (0-4) (0)                 | 0.841*                |
| <= 3 – no (%)                | 12 (75.0)            | 8 (72.7)                    |                       |
| >3 – no (%)                  | 4 (25.0)             | 3 (27.3)                    |                       |
| <b>Laboratory features</b>   |                      |                             |                       |
| Mean ± SD (missing)          |                      |                             |                       |
| Hemoglobin – g/dl            | 13.22 ± 1.56 (0)     | 13.11 ± 2.08 (1)            | 0.792*                |
| Platelets – bn/l             | 250.81 ± 51.15 (0)   | 259.5 ± 48.18 (1)           | 0.897*                |
| Creatinine – mg/dl           | 0.82 ± 0.12 (2)      | 0.9 ± 0.18 (5)              | 0.455*                |
| ALT [xULN]                   | 15.05 ± 13 (2)       | 3.38 ± 2.3 (3)              | 0.008*                |
| AST [xULN]                   | 12.88 ± 9.62 (2)     | 3.37 ± 2.2 (3)              | 0.024*                |
| GGT – U/l                    | 264.14 ± 149.74 (2)  | 361.88 ± 177.17 (3)         | 0.413*                |
| AP – U/l                     | 184.93 ± 48.18 (2)   | 301.57 ± 216.46 (4)         | 0.247*                |
| IGG – g/dl                   | 21.98 ± 7.26 (3)     | 16.1 ± 8.61 (4)             | 0.074*                |
| INR                          | 1.12 ± 0.16 (1)      | 0.99 ± 0.03 (3)             | 0.065*                |
|                              |                      |                             | * Mann-Whitney U test |
|                              |                      |                             | ** Fishers exact test |

**Table S5. Clinical characteristics of CITE-seq and snRNA-seq cohorts.**

|                              | CITE-seq           | snRNA-seq         |
|------------------------------|--------------------|-------------------|
|                              | N=10               | N=6               |
| <b>Basic characteristics</b> |                    |                   |
| Age - median (range)         | 48 (30 - 62)       | 48 (22 - 63)      |
| Sex Female – no (%)          | 7 (70.0%)          | 6 (100%)          |
| <b>Histological features</b> |                    |                   |
| mHAI Score                   |                    |                   |
| Median (range) (missing)     | 5.75 (3-11) (0)    | 7.0 (3-13) (0)    |
| <6 – no (%)                  | 5 (50.0)           | 2 (33.3)          |
| 6-9 – no (%)                 | 4 (40.0)           | 2 (33.3)          |
| 10-18 – no (%)               | 1 (10.0)           | 2 (33.3)          |
| Fibrosis score               |                    |                   |
| Median (range) (missing)     | 1.25 (0-4) (0)     | 0 (0-4) (0)       |
| <= 3 – no (%)                | 8 (80.0)           | 5 (83.3)          |
| >3 – no (%)                  | 2 (20.0)           | 1 (16.7)          |
| <b>Laboratory features</b>   |                    |                   |
| Mean ± SD (missing)          |                    |                   |
| Hemoglobin – g/dl            | 12.55 ± 1.13 (0)   | 12.9 ± 0.84 (0)   |
| Platelets – bn/l             | 236.5 ± 145.19 (0) | 304.0 ± 53.38 (0) |
| Creatinine – mg/dl           | 0.75 ± 0.17 (4)    | 0.86 ± 0.17 (2)   |
| ALT [xULN]                   | 10.02 ± 8.03 (0)   | 15.33 ± 17.40 (0) |
| AST [xULN]                   | 3.97 ± 4.61 (0)    | 10.18 ± 16.59 (0) |
| GGT – U/l                    | 112.0 ± 120.84 (0) | 180.5 ± 115.7 (0) |
| ALP – U/l                    | 95.00 ± 29.29 (0)  | 154.0 ± 56.93 (2) |
| IGG – g/dl                   | 17.64 ± 4.95 (4)   | 20.33 ± 12.77 (4) |
| INR                          | 1.0 ± 0.11 (1)     | 1.1 ± 0.36 (1)    |

**Table S6. Clinical characteristics of FACS cohorts.**

|                              | AIH               | Control          |
|------------------------------|-------------------|------------------|
|                              | N=11              | N=6              |
| <b>Basic characteristics</b> |                   |                  |
| Age - median (range)         | 54 (22 - 77)      | 52.5 (35 - 67)   |
| Sex Female – no (%)          | 7 (63.64%)        | 6 (100%)         |
| <b>Histological features</b> |                   |                  |
| mHAI Score                   |                   |                  |
| Median (range) (missing)     | 9.0 (3-16) (0)    | --               |
| <6 – no (%)                  | 1 (9.09)          |                  |
| 6-9 – no (%)                 | 5 (45.45)         |                  |
| 10-18 – no (%)               | 5 (45.45)         |                  |
| Fibrosis score               |                   |                  |
| Median (range) (missing)     | 1.0 (0-4) (0)     | 0.5 (0-1) (2)    |
| <= 3 – no (%)                | 10 (90.91)        | 4 (100)          |
| >3 – no (%)                  | 1 (9.09)          | 0 (0)            |
| <b>Laboratory features</b>   |                   |                  |
| Mean ± SD (missing)          |                   |                  |
| Hemoglobin – g/dl            | 13.6 ± 1.62 (0)   | --               |
| Platelets – bn/l             | 179.0 ± 78.83 (0) | --               |
| Creatinine – mg/dl           | 0.82 ± 0.16 (0)   | --               |
| ALT [xULN]                   | 9.10 ± 6.94 (0)   | 1.19 ± 4.38 (0)  |
| AST [xULN]                   | 5.77 ± 5.69 (0)   | 0.66 ± 3.26 (0)  |
| GGT – U/l                    | 141.0 ± 94.04 (0) | 47.5 ± 32.92 (0) |
| ALP – U/l                    | 102.0 ± 75.64 (0) | --               |
| IGG – g/dl                   | 22.71 ± 9.10 (0)  | --               |
| INR                          | 1.0 ± 0.11 (0)    | --               |

**Table S7. Clinical characteristics of spatial *in situ* RNA expression cohorts.**

|                              | AIH                | Control           |
|------------------------------|--------------------|-------------------|
|                              | N=6                | N=3               |
| <b>Basic characteristics</b> |                    |                   |
| Age - median (range)         | 38.5 (28 - 73)     | 39 (35 - 49)      |
| Sex Female – no (%)          | 5 (83.3%)          | 0 (0%)            |
| <b>Histological features</b> |                    |                   |
| mHAI Score                   |                    |                   |
| Median (range) (missing)     | 11.5 (10-13) (0)   | 0 (0-1) (0)       |
| <6 – no (%)                  | 0 (0)              | 3 (100)           |
| 6-9 – no (%)                 | 0 (0)              | 0 (0)             |
| 10-18 – no (%)               | 6 (100)            | 0 (0)             |
| Fibrosis score               |                    |                   |
| Median (range) (missing)     | 1.5 (0-4) (0)      | 0 (0-0) (0)       |
| <= 3 – no (%)                | 4 (66.7)           | 3 (100)           |
| >3 – no (%)                  | 2 (33.3)           | 0 (0)             |
| <b>Laboratory features</b>   |                    |                   |
| Mean ± SD (missing)          |                    |                   |
| Hemoglobin – g/dl            | 13.35 ± 0.76 (0)   | 16.3 ± 0.6 (0)    |
| Platelets – bn/l             | 166.5 ± 117.61 (0) | 204.0 ± 82.53 (0) |
| Creatinine – mg/dl           | 0.70 ± 0.47 (0)    | 1.03 ± NA (2)     |
| ALT [xULN]                   | 24.71 ± 17.41 (0)  | 1.24 ± 0.25 (0)   |
| AST [xULN]                   | 23.0 ± 17.16 (0)   | 0.84 ± 0.25 (0)   |
| GGT – U/l                    | 135.5 ± 67.7 (0)   | 119.0 ± 44.84 (0) |
| ALP – U/l                    | 165.5 ± 79.58 (0)  | 71.0 ± 20.82 (0)  |
| IGG – g/dl                   | 15.49 ± 7.22 (0)   | 11.8 ± 0.42 (1)   |
| INR                          | 1.2 ± 0.33 (0)     | 1.05 ± 0.07 (1)   |

**Table S8. Gene list for residency score.**

| <b>CD4+ T cells</b> | <b>CD8+ T cells</b> |
|---------------------|---------------------|
| CD69                | CD69                |
| CA10                | CA10                |
| IL17F               | IL17A               |
| IL2                 | CXCL13              |
| CDHR1               | SCUBE1              |
| IL21                | HASPIN              |
| IL10                | ITGA1               |
| IL23R               | CXCR6               |
| CXCL13              | ATP8B4              |
| CXCR6               | CSF1                |
| KCNK5               | ITGAE               |
| ITGA1               | CPNE7               |
| JAG2                | IL10                |
| SRGAP3              | SPRY1               |
| TOX2                | MCAM                |
| CH25H               | RGS1                |
| NEK10               | KCNQ3               |
| TMEM200A            | DAB2IP              |
| MYO1B               | TRPM2               |
| PLXDC1              | KCNK5               |
| IKZF3               | IL23R               |
| GFOD1               | PELO                |
| CRTAM               | COL5A1              |
| DUSP6               | IRF4                |
| RGS1                | FSD1                |
| TP53I11             | IL17RE              |
| GFI1                | ADAM12              |
| IFNG                | CRTAM               |
| SLC7A5              | ARHGAP18            |
| GCNT4               | CCR1                |
|                     | JAML                |
|                     | ICOS                |
|                     | TMIGD2              |
|                     | TP53INP1            |
|                     | BMF                 |
|                     | CD9                 |
|                     | RIMS3               |
|                     | DUSP6               |
|                     | CCR6                |
|                     | GZMB                |
|                     | ZNF683              |

**Table S9. Gene list for migratory score.**

| CD4+ T cells | CD8+ T cells |
|--------------|--------------|
| RIPOR2       | PXN          |
| STK38        | FLNA         |
| GRASP        | CYB561       |
| KLF3         | CD300A       |
| SAMD3        | TSPAN32      |
| GABBR1       | RASA3        |
| FRY          | ADGRG5       |
| ARHGEF11     | TGFBR3       |
| VIPR1        | SAMD3        |
| BAIAP3       | PELI2        |
| MFGE8        | C11orf21     |
| SBK1         | RASGRP2      |
| HAPLN3       | SYNE1        |
| TTC16        | GK5          |
| CX3CR1       | SSX2IP       |
| USP46        | STK38        |
| PLXNA4       | FGR          |
| NSG1         | SSBP3        |
| DSEL         | CFH          |
| CNTNAP1      | ADAMTS10     |
| VSIG1        | MTSS1        |
| RGMB         | KLF3         |
| TTYH2        | KLF2         |
| EPHA4        | SVIL         |
| TNFRSF11A    | CACNA2D2     |
| MUC1         | RIPOR2       |
| CR1          | SBK1         |
| E2F2         | PATL2        |
| KLF2         | TMCC3        |
| EDA          | KIR2DS4      |
| KRT73        | HPCAL4       |
| ZNF462       | VCL          |
| RAP1GAP2     | TTC16        |
| S1PR1        | PDZD4        |
| NPDC1        | DCHS1        |
| KLF3-AS1     | EBF4         |
| ISM1         | OSBPL5       |
| TSPAN18      | FZD4         |
| KCTD15       | GNLY         |
| KRT72        | NHSL2        |
| SEMA5A       | TSPAN18      |
| WNT7A        | ME3          |
| SOX13        | MSX2P1       |
| FUT7         | ZNF711       |
| PTGDS        | NSG1         |
| PI16         | FCGR3A       |
| SEMA3G       | GPA33        |
| SYT4         | COL6A2       |
|              | CXCR2        |
|              | TTYH2        |
|              | AGPAT4       |
|              | TKTL1        |
|              | SELP         |
|              | LILRB1       |
|              | ITGAM        |
|              | LOXL4        |
|              | KLF3-AS1     |
|              | TFCP2L1      |
|              | C1orf21      |
|              | SLCO4C1      |
|              | NUAK1        |
|              | PALLD        |
|              | DNAI2        |
|              | SOX13        |
|              | S1PR1        |
|              | SELL         |
|              | PLEKHG3      |
|              | ADGRG1       |
|              | SPTB         |
|              | ZNF365       |
|              | PCDH1        |
|              | NPDC1        |
|              | KRT73        |
|              | KRT72        |
|              | ASCL2        |
|              | TAFA1        |
|              | SGCD         |
|              | LAIR2        |
|              | EFHC2        |
|              | RAP1GAP2     |
|              | NME8         |
|              | PODN         |
|              | SH3RF2       |
|              | KIF19        |
|              | PTGDS        |
|              | EPHX4        |
|              | PRSS23       |
|              | KIR3DX1      |
|              | CX3CR1       |
|              | SLC1A7       |
|              | FGFBP2       |
|              | LRFN2        |
|              | DGKK         |

**Table S10. Gene list for a.a. score.**

|           |
|-----------|
| RUNX3     |
| JUN       |
| RGS1      |
| CD8A      |
| DUSP2     |
| NR4A2     |
| PDCD1     |
| CXCR6     |
| TIGIT     |
| ZBTB38    |
| GZMK      |
| GZMA      |
| CD74      |
| FYN       |
| IFNGR1    |
| TOX       |
| GABARAPL1 |
| IFNG      |
| ALOX5AP   |
| CCL5      |
| IKZF3     |
| CST7      |
| GZMM      |
| ZFP36     |

## Supplementary figures

Supplementary Fig. 1

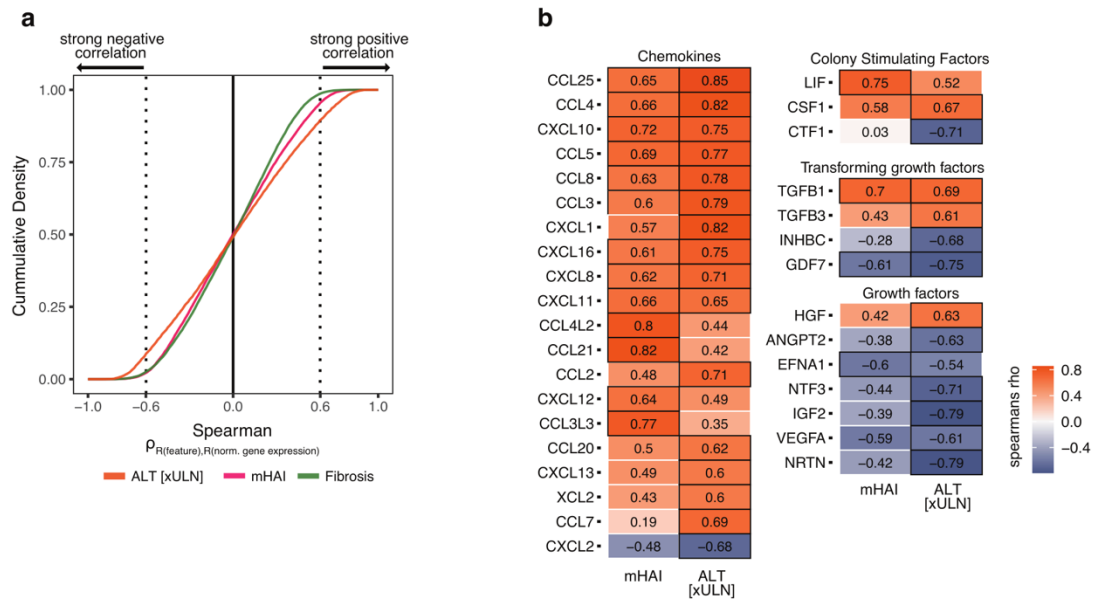


**Fig. S1. Gene - feature correlation of patients with AIH identified by bulk mRNA sequencing.** (a) Distribution of  $r_s$  values across all genes and the features ALT, mHAI, Fibrosis Score in patients with AIH depicted by cumulative density.  $r_s \geq 0.6$  or  $< -0.6$  defined as strong correlation. (b) Heatmap of strongly correlating chemokines, colony stimulating factors, transforming growth factors and growth factors.

Supplementary Fig. 2

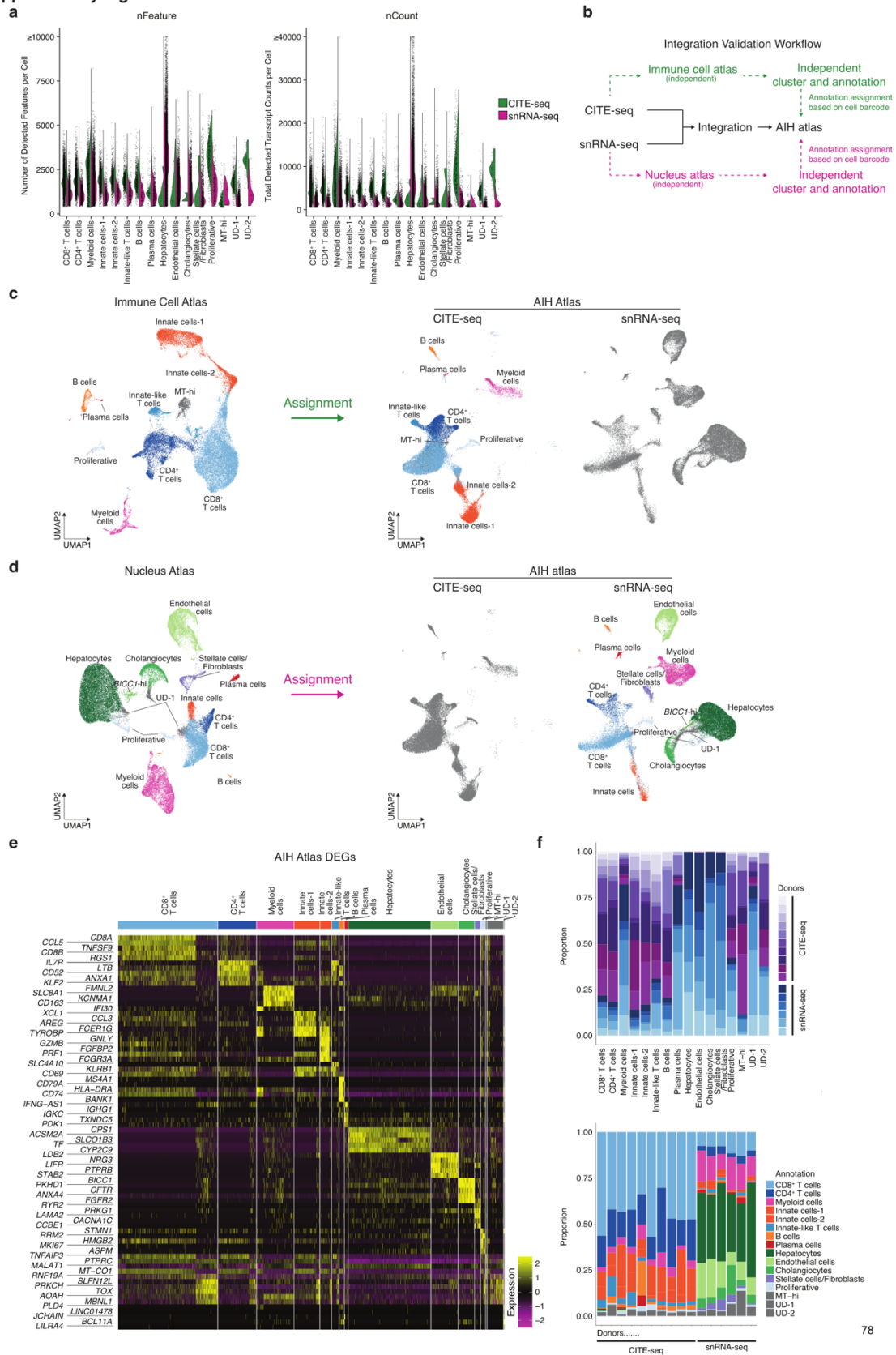


**Fig. S2. CITE-seq and snRNA-seq integration validation and cluster annotation.** (a) Violin plots for quality control: library size (nFeature) and total transcript counts (nCount) by cell type and sequencing approach. Values of nFeature exceeding 10,000 were capped at 10,000 on

the y-axis for visualization, and values of nCount exceeding 40,000 were capped at 40,000 on the y-axis for visualization. **(b)** Schematic representation of the validation strategy for integrating CITE-seq and snRNA-seq datasets. **(c)** Left: Cell type annotation of the immune cell atlas performed independently (CITE-seq, n=10). Right: Annotation transfer to the AIH atlas using barcode matching. **(d)** Left: Cell type annotation of the nucleus atlas performed independently (snRNA-seq, n=6) (UD: Un-defined). Right: Annotation transfer to the AIH atlas using barcode matching. **(e)** Heatmap of scaled expression values of the top 5 DEGs per cell type in CITE-seq and snRNA-seq integrated AIH atlas. UD-1 and UD-2 are not explicitly labelled in Fig. 2c, but are represented in grey (UD: Un-defined). **(f)** Top: Distribution of samples/datasets per cell type; Bottom: Distribution of cell type per samples/datasets.

Supplementary Fig. 3

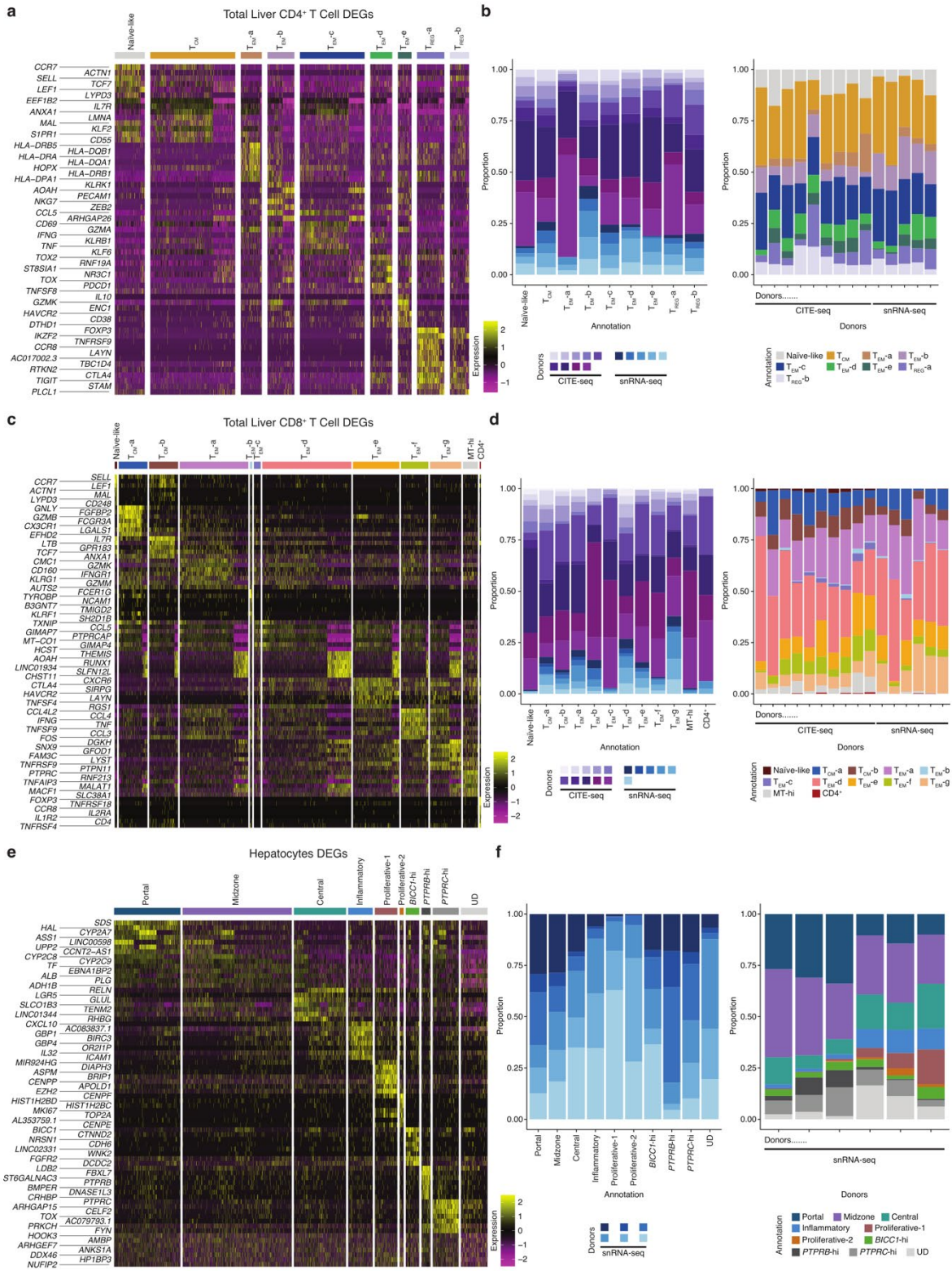


**Fig. S3. Zoom-in analysis of CD4<sup>+</sup> T cells, CD8<sup>+</sup> T cells, and Hepatocytes from the AIH atlas: subcluster specific differential expression genes and sample contribution. (a, c, e) Heatmap of scaled expression values of the top 7 DEGs per CD4<sup>+</sup> T cells (a) CD8<sup>+</sup> T cells**

(c) and Hepatocytes (e) subtypes. RPL and RPS genes are not displayed. (RPL: Ribosomal Protein L; RPS: Ribosomal Protein S) (**b**, **d**, **f**) Left: Contribution of each sample to the subtypes. Right: Contribution of subtypes to each sample.

**Supplementary Fig. 4**

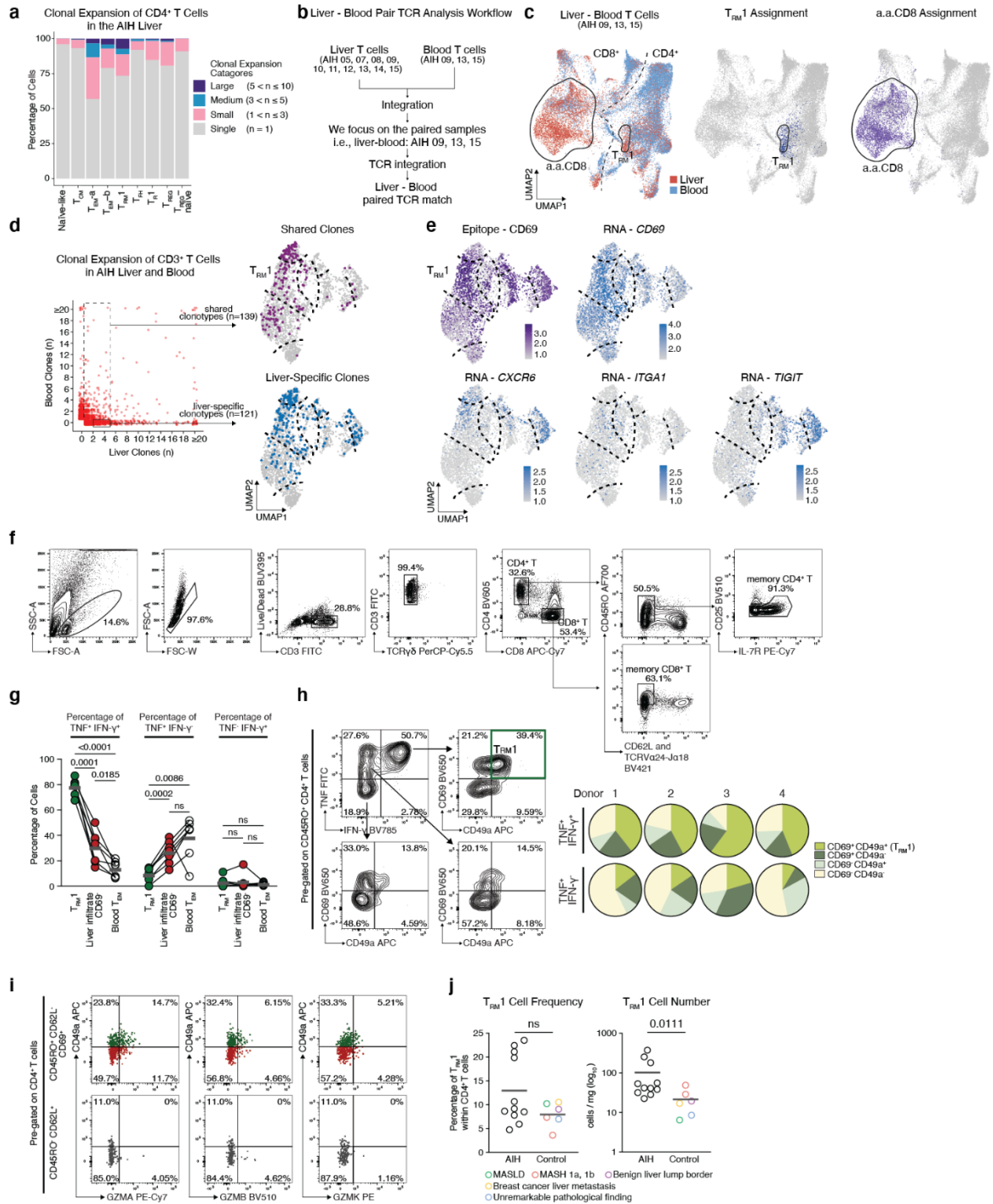


**Fig. S4. Proinflammatory profile of T<sub>RM</sub>1 cells.** (a) Bar chart depicting clonal expansion percentages within each liver CD4<sup>+</sup> T cell cluster. (b) Schematic representation of the TCR analysis strategy. (c) Left: UMAP of liver and paired blood T cells, coloured by organ source. Right: T<sub>RM</sub>1 cells (corresponding to Fig. 2d, T<sub>EM</sub>-c) and a.a.CD8<sup>+</sup> T cells (corresponding to Fig. 2e, T<sub>EM</sub>-a to -g) are shown after annotation transfer of T<sub>RM</sub>1 and a.a.CD8<sup>+</sup> T cells from Fig. 2d (T<sub>EM</sub>-c) and Fig. 2e (T<sub>EM</sub>-a to -g) to this liver - paired blood T cell UMAP using barcode matching. (d) Left: Clonal expansion of CD3<sup>+</sup> T cells, in the livers and paired blood (liver CITE-seq: n = 3; paired blood CITE-seq: n = 3). The X-axis and Y-axis represent liver and blood

clones, respectively, with clone counts  $\geq 20$  truncated to 20 for visualization. Right: UMAP of CD4<sup>+</sup> T cells highlighting clones shared between the liver and blood with frequencies of  $1 \leq n \leq 5$  (top) and liver-specific clones with frequencies of  $2 \leq n \leq 5$  (bottom). (e) UMAP of the expression of marker epitope and genes used for T<sub>RM1</sub> identification. (f) Flow cytometry gating strategy for the identification of T<sub>RM1</sub> and a.a.CD8<sup>+</sup> T cells by surface staining. Auto-fluorescence events were excluded between the third and fourth dot plots by combining multiple fluorescence channels. (g) Frequencies of three distinct TNF and IFN- $\gamma$  expression combinations across the indicated CD4<sup>+</sup> populations in 7 AIH donors. The gating strategies for the indicated populations is shown in Fig.3f left. TNF and IFN- $\gamma$  detection were performed after in vitro stimulation. Each dot represents a single donor, with frequencies of different populations from the same donor connected by lines. Grey lines represent mean values. Significant differences are determined by RM one-way ANOVA, Tukey's multiple comparisons test. (h) Representative flow cytometry plots (left) and pie chart quantifications (right) depicting the contribution of indicated cell populations across different TNF and IFN- $\gamma$  expression profiles. CD45RO<sup>+</sup> CD4<sup>+</sup> T cells were pre-gated on TCR $\alpha\beta$ <sup>+</sup> TCRV $\alpha$ 24-J $\alpha$ 18<sup>-</sup> live, singlet lymphocytes. (i) Flow cytometry plots illustrating the expression patterns of selected granzymes in the indicated CD4<sup>+</sup> populations (n = 1). CD4<sup>+</sup> T cells were pre-gated on TCR $\alpha\beta$ <sup>+</sup>, live, singlet lymphocytes. Auto-fluorescence events were excluded by combining multiple fluorescence channels. Granzymes were detected by intracellular staining without prior in vitro stimulation. (j) Frequencies (left) of T<sub>RM1</sub> cells within total CD4<sup>+</sup> T cells are shown to illustrate the basis for calculating absolute T<sub>RM1</sub> cell numbers (right), which were normalized per gram of liver tissue in patients with AIH (n=11) and controls (n=6), as measured by flow cytometry. The gating strategy for T<sub>RM1</sub> cells is shown in Fig. S4f followed by Fig. 3e. Weight normalized T<sub>RM1</sub> cell numbers were further log<sub>10</sub> transformed for statistical analysis, while the y-axis displays the original untransformed values. Each dot represents a single donor, and the bar represents the mean. Statistical differences are determined by unpaired t-test. Panels a - e were based on the AIH atlas, whereas panels f - j were based on the FACS dataset.

Supplementary Fig. 5

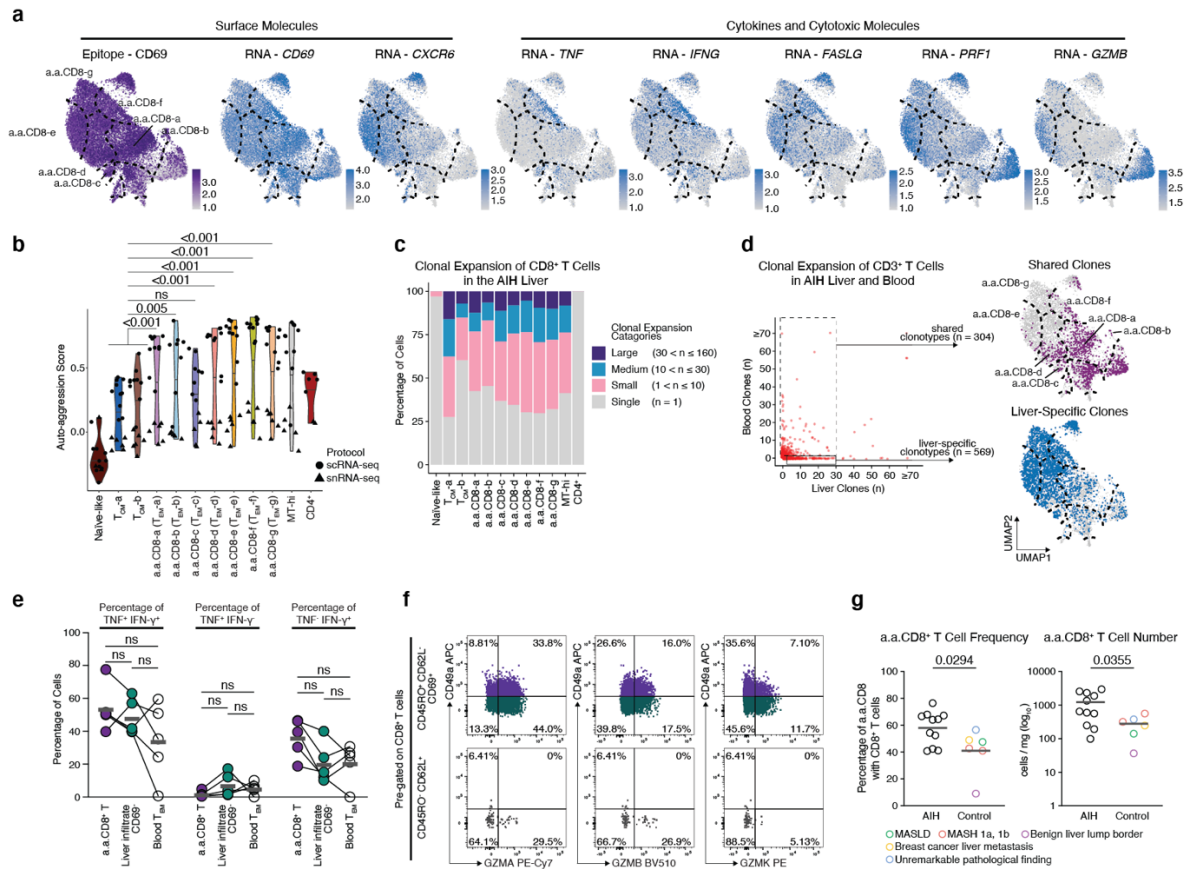


**Fig. S5. Cytotoxic profile of a.a.CD8<sup>+</sup> T cells.** (a) UMAP showing the expression of marker epitope and genes characteristic of liver a.a.CD8<sup>+</sup> T cells. (b) a.a. scores for all CD8<sup>+</sup> T cell subclusters are shown as the average per sample. P values were determined on the cluster- and sample- averaged scores using a mixed linear effects model with Dunnet's test post hoc. Two T<sub>CM</sub> clusters were merged for statistical analysis but are displayed as separate clusters for visualization. (c) Bar chart depicting clonal expansion percentages within each liver CD8<sup>+</sup> T cell clusters. (d) Left: Clonal expansion of CD3<sup>+</sup> T cells, in the livers and paired blood (liver CITE-seq: n = 3; paired blood CITE-seq: n = 3). The X-axis and Y-axis represent liver and blood clones, respectively, with clone counts  $\geq 70$  truncated to 70 for visualization. Right: UMAP of CD8<sup>+</sup> T cells highlighting clones shared between the liver and blood with frequencies of  $1 \leq n \leq 30$  (top) and liver-specific clones with frequencies of  $2 \leq n \leq 30$  (bottom). (e) Frequencies of distinct TNF and IFN- $\gamma$  expression patterns across the indicated CD8<sup>+</sup> populations in 5 AIH donors. The gating strategies for the indicated CD8<sup>+</sup> populations are shown in Fig.3I left. TNF and IFN- $\gamma$  detection were performed after in vitro stimulation. Each dot represents a single donor, with frequencies of different populations from the same donor connected by lines. Grey lines represent mean values. Statistical differences are determined by RM one-way ANOVA, Tukey's multiple comparisons test. (f) Flow cytometry plots illustrating the expression patterns of selected granzymes in the indicated CD8<sup>+</sup> populations (n = 1). CD8<sup>+</sup> T cells were pre-gated on TCR $\alpha\beta$ <sup>+</sup>, live, singlet lymphocytes. Auto-fluorescence events were

excluded by combining multiple fluorescence channels. Granzymes were detected by intracellular staining without prior in vitro stimulation. **(g)** Frequencies (left) of a.a.CD8<sup>+</sup> T cells within total CD8<sup>+</sup> T cells are shown to illustrate the basis for calculating absolute a.a.CD8<sup>+</sup> T cell numbers (right), which were normalized per gram of liver tissue in patients with AIH (n=11) and controls (n=6), as measured by flow cytometry. The gating strategy for a.a.CD8<sup>+</sup> T cells is shown in Fig. S4f followed by Fig.3k. Weight normalized a.a.CD8<sup>+</sup> T cell numbers were further log<sub>10</sub> transformed for statistical analysis, while the y-axis displays the original untransformed values. Each dot represents a single donor, and the bar represents the mean. Statistical differences are determined by unpaired t-test. Panels a - d were based on the AIH atlas, whereas panel e - g were based on the FACS dataset.

Extended Data Fig. 6

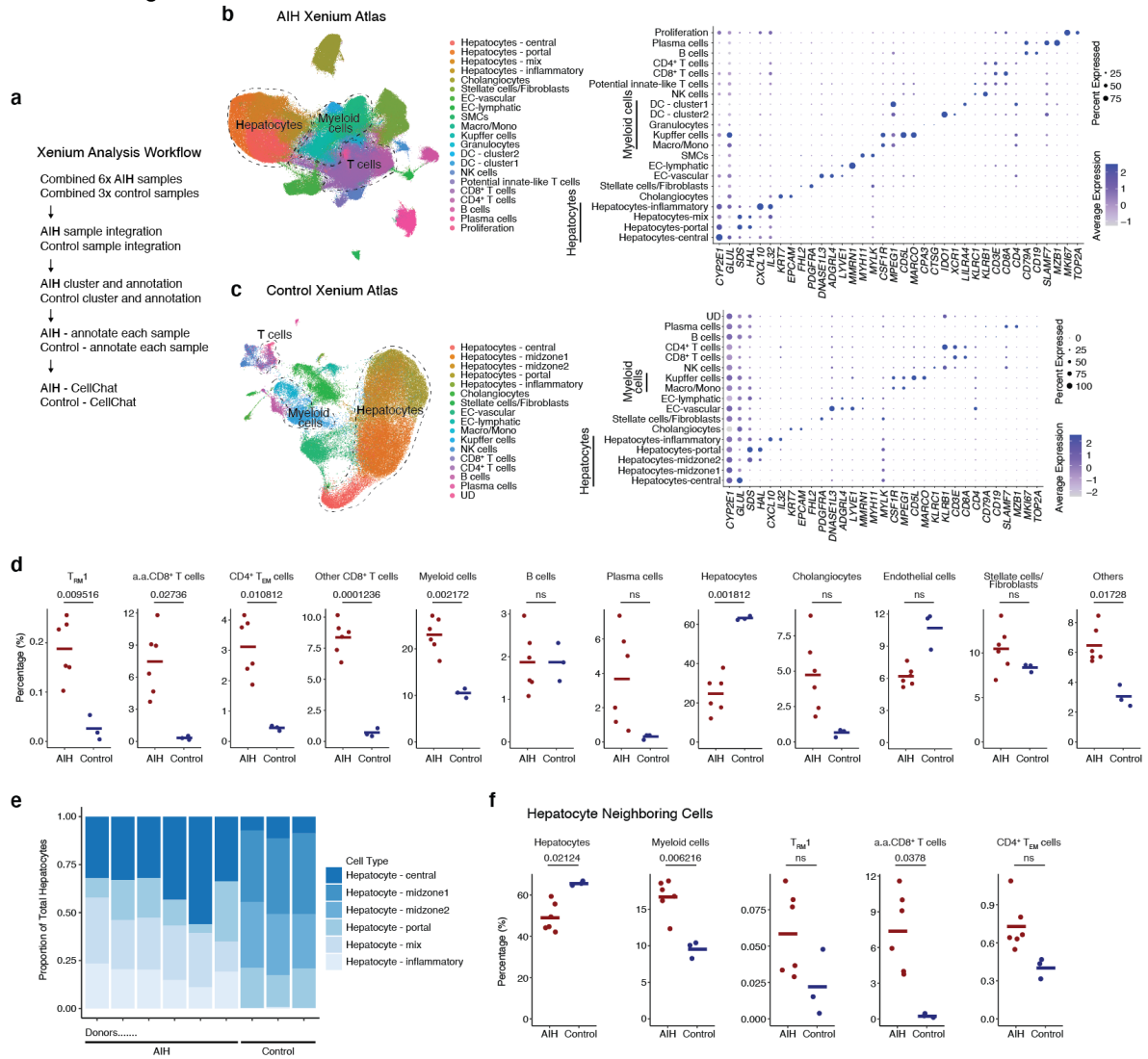


**Fig. S6. Comparison of the spatial frequency and distribution of cells in AIH and control liver samples, based on spatial in situ RNA expression dataset. (a)** Schematic representation of spatial in situ RNA expression analysis workflow. **(b)** Left: UMAP of integrated spatial in situ RNA expression data of AIH patients (n = 6). Right: Dot plots showing expression of marker genes in indicated cell types. (NK cells: natural killer cells; DC: dendritic cells; SMC: smooth muscle cells) **(c)** Left: UMAP of integrated spatial in situ RNA expression data of control samples (n = 3). Right: Dot plots showing expression of marker genes in indicated cell types. **(d)** Percentage of indicated clusters within total cells per biopsy in AIH and control. Each dot represents a single donor, and the bar indicating the mean. Significant differences were determined using a t-test with Bonferroni correction for multiple comparisons. **(e)** Proportions of hepatocyte populations in AIH and control samples. **(f)** Quantification of hepatocytes neighbouring cells. Each dot represents a single donor, and the bar indicating the mean. Significant differences are indicated by t-test with Bonferroni correction for multiple hypothesis testing.

Supplementary Fig. 7

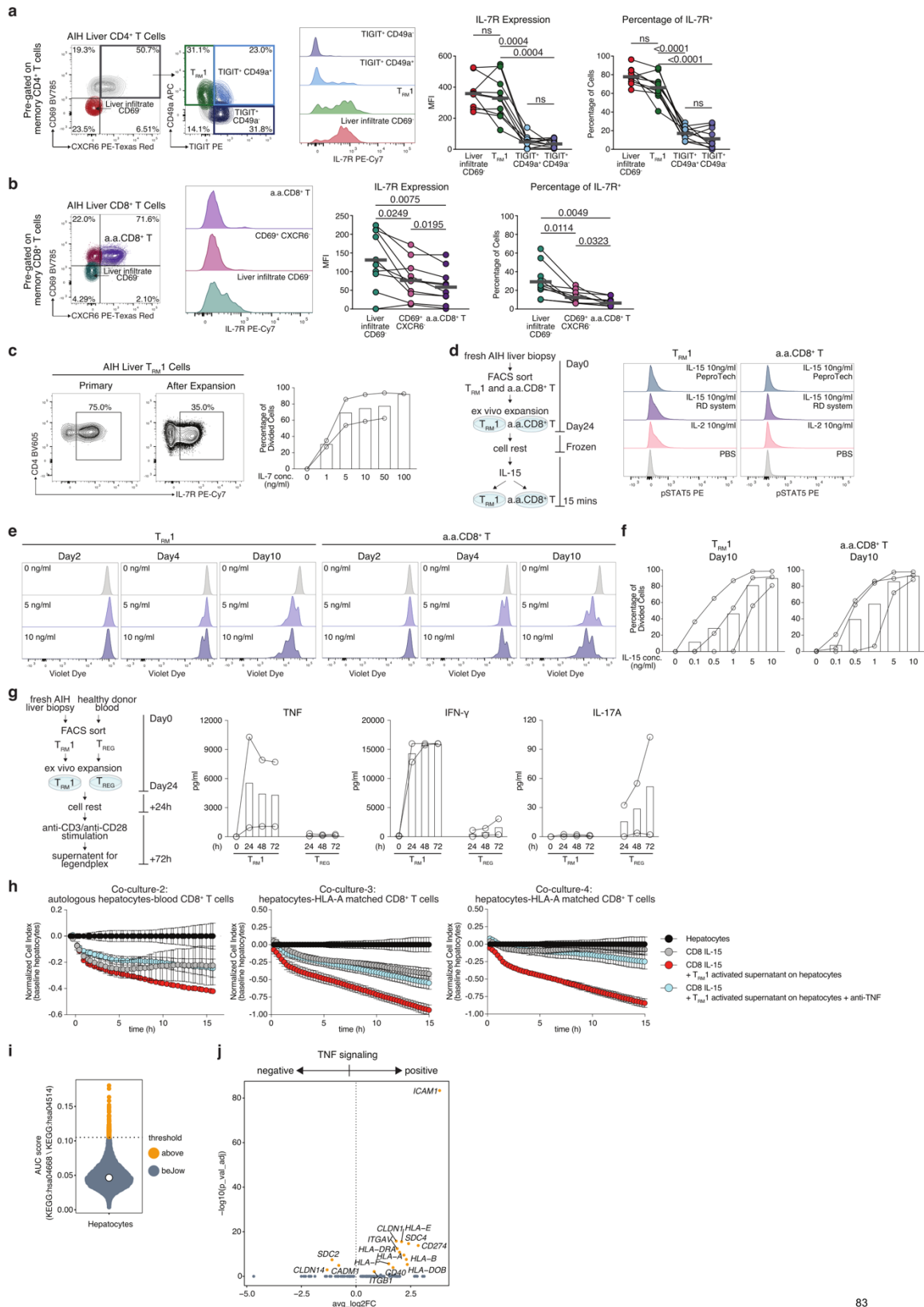


**Fig. S7. In vitro validation of IL-7, IL-15 and TNF effects on liver T cells. (a-b) Left:** Representative flow cytometry plots illustrating the gating strategy for the indicated CD4<sup>+</sup> (a) and CD8<sup>+</sup> (b) T cell populations from patients with AIH; gating for memory CD4<sup>+</sup> and CD8<sup>+</sup> T

cells is shown in Fig. S4f. Middle: Representative histograms showing the MFI of IL-7R across the indicated liver CD4<sup>+</sup> (a) and CD8<sup>+</sup> (b) T cell populations in 10 AIH donors. Each dot represents a single donor, and MFI/frequency of different populations from the same donor is connected by lines. Grey lines represent mean values. Significant differences are determined by RM one-way ANOVA, Tukey's multiple comparisons test. (c) Left: Representative flow cytometry plot showing IL-7R expression in T<sub>RM</sub>1 cells isolated from AIH liver before and after ex vivo clonal expansion. Right: Bar plot illustrating the proliferation effect of IL-7 on T<sub>RM</sub>1 cells at indicated doses (AIH patients n = 2). Each dot represents a single donor, with cells treated with different IL-7 concentration from the same donor connected by lines. Bars indicate the mean. (d) Left: Schematic representation of IL-15R activation detection strategy. Right: Histogram showing the MFI distribution of STAT5 phosphorylation (pSTAT5) across AIH liver derived T<sub>RM</sub>1 and a.a.CD8<sup>+</sup> T cells under the specified conditions (n=1). This analysis aims to detect the phosphorylation of STAT5, a downstream component of IL-15 signalling pathway, to indirectly validate IL-15R activation. (e) CellTrace Violet histograms showing proliferation of AIH liver derived T<sub>RM</sub>1 and CD8<sup>+</sup> T cells under indicated conditions (n=1). Due to the multiple roles of IL-15 on T cells, this analysis aims to determine if the proliferative effect of IL-15 is time dependent. The results show that the proliferative effect begins only after day 4 of ex vivo exposure. (f) Bar plot illustrating the proliferation effect of IL-15 on AIH liver derived T<sub>RM</sub>1 and a.a.CD8<sup>+</sup> T cells at different doses (n = 3) over 10 days. Each dot represents a single donor, with cells treated with different IL-15 concentration from the same donor connected by lines. Bars indicate the mean. (g) Left: Schematic representation of the validation strategy for the cytokine profile of AIH liver-derived T<sub>RM</sub>1 cells following ex vivo clonal expansion. Healthy donor blood-derived T<sub>REG</sub>-like cells were included as control. CD25<sup>+</sup> IL7R<sup>-</sup> CD45RO<sup>+</sup> CD62L<sup>-</sup> CD4<sup>+</sup> TCRαβ<sup>+</sup> live, singlet lymphocytes were defined as T<sub>REG</sub>-like cells in the FACS-sorting gating strategy. Right: bar plots illustrating the selected cytokine profiles of T<sub>RM</sub>1 and T<sub>REG</sub>-like cells following anti-CD3/anti-CD28 stimulation at the indicated time points. Supernatants were analysed using the LegendPlex assay as the readout. (T<sub>RM</sub>1 from AIH livers, n = 2; T<sub>REG</sub>-like cells from healthy donor blood, n = 2). Each dot represents the mean of duplicate measurements, with data from the same donor at different time points connected by lines. Bars indicate the mean. (h) Co-culture-2: Real-time cell impedance analysis over 15h showing auto-aggressive activity of autologous blood CD8<sup>+</sup> T cells against primary human hepatocytes under the indicated conditions. Hepatocytes were co-cultured with CD8<sup>+</sup> T cells (grey), or pre-treated with supernatant from anti-CD3/anti-CD28 activated T<sub>RM</sub>1 cells in the absence (red) or presence of anti-TNF (blue). Baseline hepatocytes are shown in black. Primary hepatocytes and autologous blood CD8<sup>+</sup> T cells were obtained from one healthy donor distinct from the donor used in Fig.5f. T<sub>RM</sub>1 cells were isolated from the liver of the same AIH donor used in Fig.5f. Co-culture-3 and -4: Primary hepatocytes were derived from a third healthy donor co-

cultured with blood CD8<sup>+</sup> T cells from two HLA-A matched donors, respectively. T<sub>RM</sub>1 cells were isolated from the liver of one AIH donor distinct from the donor used in co-culture-1 and -2. Auto-aggression was assessed by hepatocyte viability and quantified using xCELLigence. Each dot represents the mean of triplicates for the indicated condition at the specified time point, with bars indicating the SD. (i) Hepatocyte TNF signalling score, based on the AIH atlas. The distribution threshold of the AUC values were marked and cells above and below were coloured with orange and grey, respectively. (j) Volcano plot of hepatocyte cell adhesion genes differentially expressed between cells above and below the TNF signalling score threshold of Fig. S7i.

Supplementary Fig. 8

a

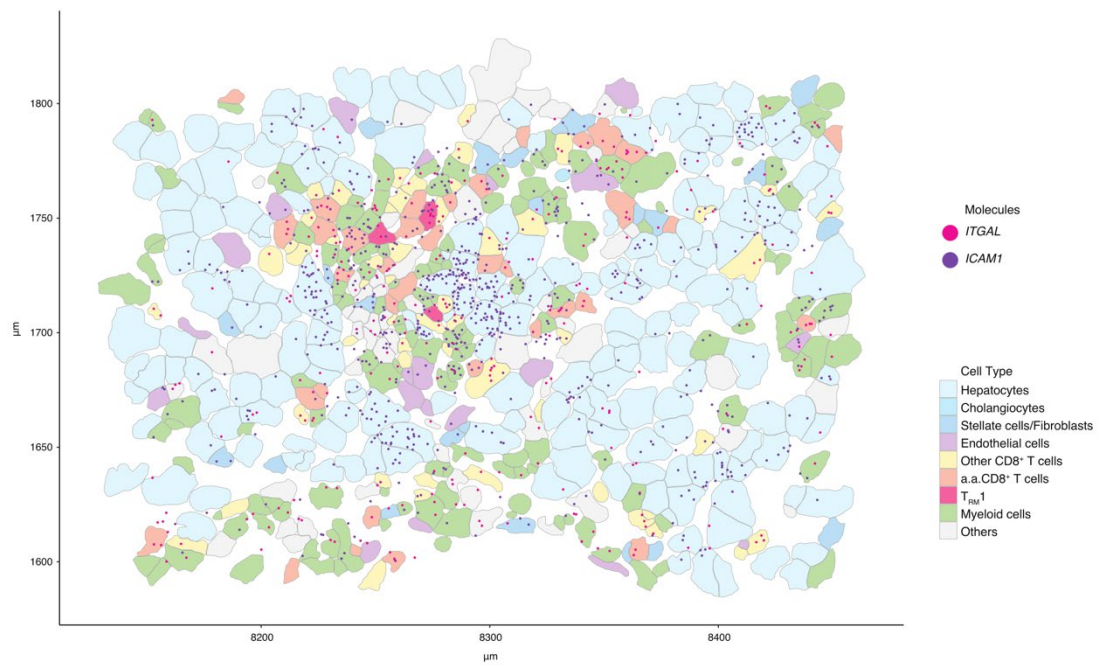
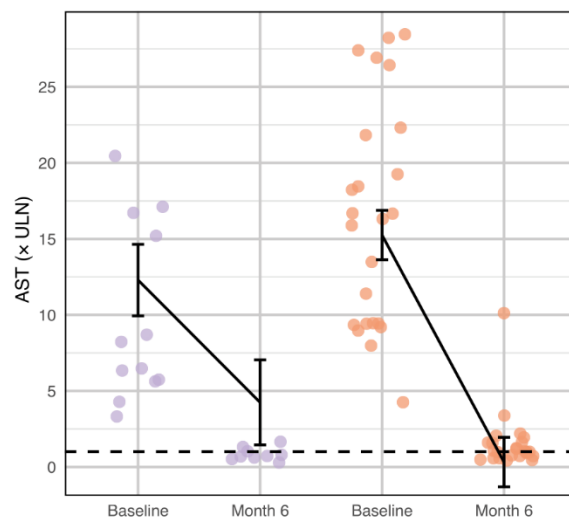


**Fig. S8. Spatial distribution of cells showing *ICAM1* and *ITGAL* expression pattern at interphase hepatitis. (a)** Spatial distribution of cells coloured by cell type, with *ICAM1* and *ITGAL* RNA expression overlaid.

Supplementary Figure 9

a



b

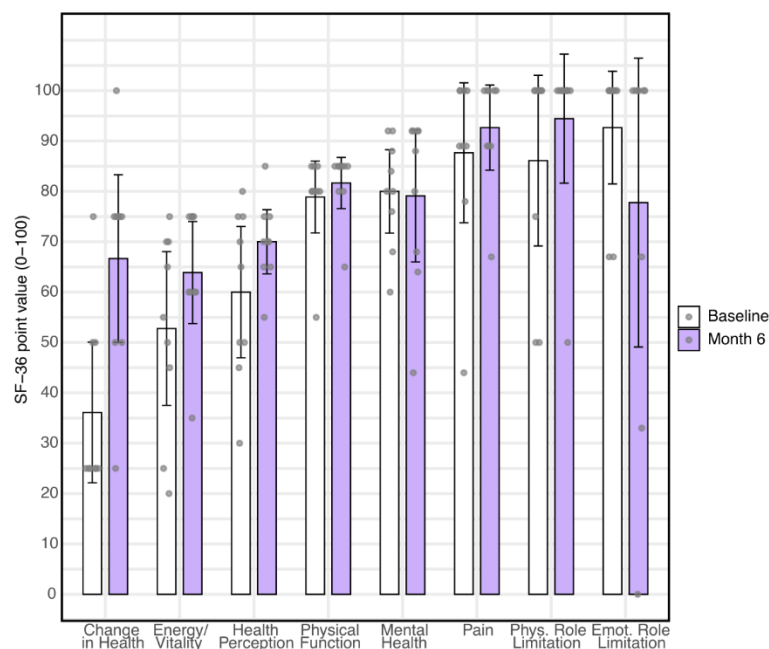


**Fig. S9. Additional outcome measurements of the AIH-MAB trial.** (a) Comparison of AST (times upper limit of normal, xULN) between baseline and month 6, separated by treatment (IFX [individual patients depicted by orange circles], n=12 vs. PSM-matched cohort, receiving standard care [SoC, purple circles], n=24). Black lines and error bars indicate respective estimated marginal means (EMMs) and their respective 95% confidence intervals (CI) of the linear mixed-effects model analyses. (b) Health-related Quality of life (HRQoL)

measurements of n=9 patients in the trial as shown per category of the Short Form 36 (SF-36) questionnaire between baseline and month 6 (point values from 0-100, 100 points indicate absence of HRQoL impairments). Dots represent individual patients, bars represent means, error bars depict respective  $\pm$  95% confidence intervals.

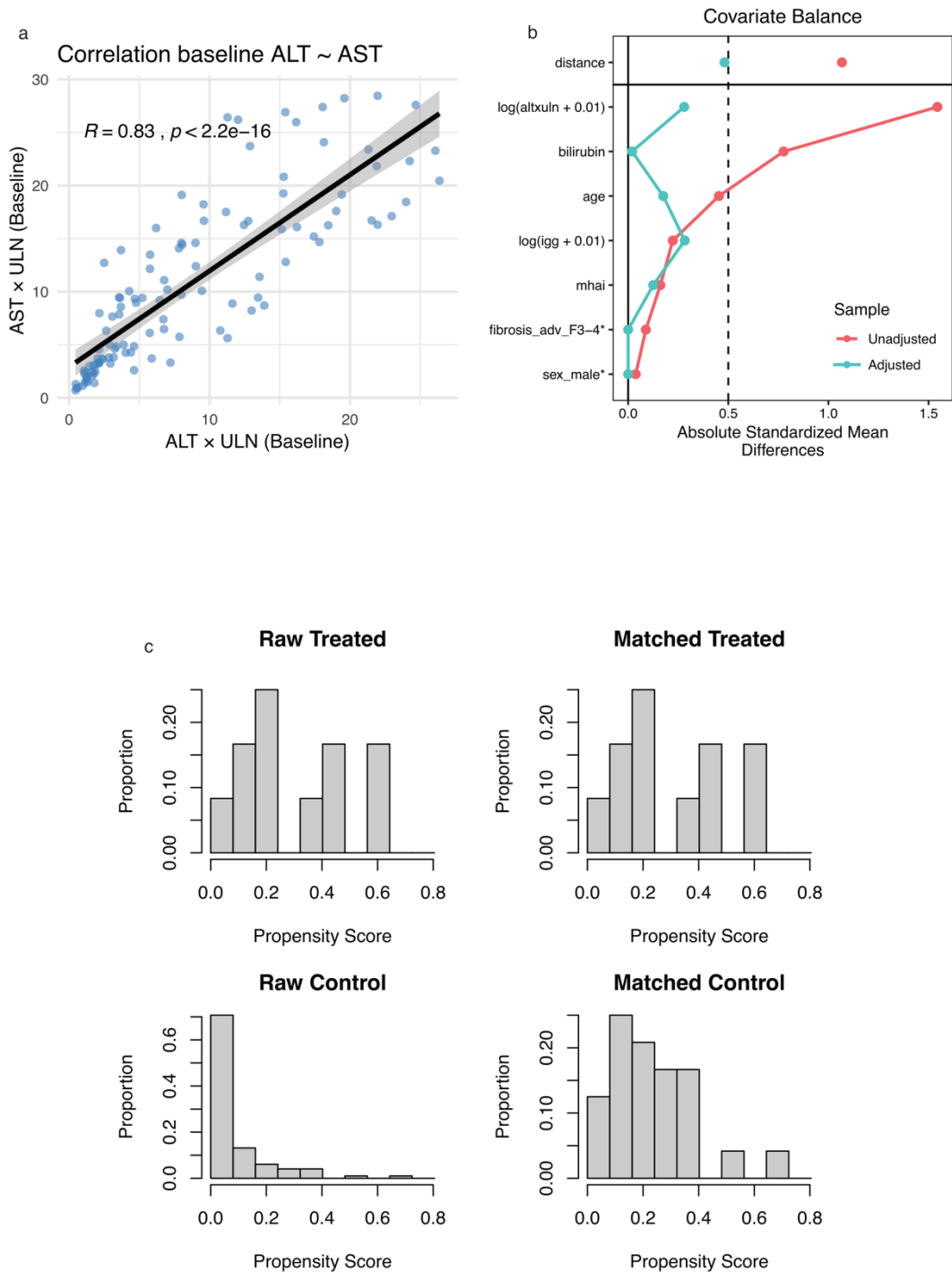


**Fig. S10. Baseline correlation and propensity score matching diagnostics** for the comparison of the clinical trial cohort and the standard of care cohort from the prospective RLIVER registry. (a) Pearson Correlation between baseline ALT and AST values. Scatterplot showing the strong linear association between baseline ALT and AST expressed as multiples of the upper limit of normal ( $\times$ ULN). (b) Covariate balance before and after propensity score matching. Absolute standardized mean differences (SMDs) for each covariate are displayed before (unadjusted, pink line) and after matching (adjusted, blue line). (c) Propensity score

distributions before and after matching. Histograms showing the distribution of propensity scores for treated (IFX) and control (SoC) individuals before (left panels) and after (right panels) 1:2 nearest-neighbor matching with exact matching on sex and fibrosis stage. Matching achieved overlap between groups, supporting adequate comparability of baseline covariates.